NUREG/CR-1314

Gravity Reflood Oscillations in a Pressurized Water Reactor

Prepared by Y. L. Cheung, P. Griffith

Department of Mechanical Engineering
Massachusetts Institute of Technology

Prepared for
U. S. Nuclear Regulatory
Commission

Available from

GPO Sales Program
Division of Technical Information and Document Control
U. S. Nuclear Regulatory Commission
Washington, D. C. 20555

and

National Technical Information Service
Springfield, Virginia 22161

NUREG/CR-1314
R2

Gravity Reflood Oscillations in a Pressurized Water Reactor

Manuscript Completed: December 1979
Date Published: February 1980

Prepared by
Y. L. Cheung, P. Griffith

Department of Mechanical Engineering
Massachusetts Institute of Technology
Boston, MA 02139

Prepared by
Division of Reactor Safety Research
Office of Nuclear Regulatory Research
U.S. Nuclear Regulatory Commission
Washington, D.C. 20555
NRC FIN No. A-4060

ABSTRACT

The thermal-hydraulics of reflood oscillations in a pressurized water reactor is studied. Violent steam generation beneath the core water level and subsequent expulsion of the coolant are proposed as the physical mechanisms responsible for driving the oscillations. A computer model of the gravity reflood process is formulated based on a simplified boiling curve and one-dimensionl fluid mechanics. In general, model calculations compare favorably with experiments. The core coolant level, however, cannot be calculated with certainty because the model does not account, in sufficient details, for interactions beyond the reactor core. Calculated vapor velocities at the core exit indicate that draining of carryover coolant from the upper plenum is possible.

TABLE OF CONTENTS

LIST OF FIGURES

NOMENCLATURE

A_c	Core flow area
A_{BP}	Bott.m plenum flow area
A_d	Downcomer flow area
A_l	Loop piping flow area
A_w	Wall surface area
E	Energy
g	Acceleration due to gravity
h	Heat transfer coefficient
H	Specific enthalpy
k	Thermal conductivity
K_c	Resistance coefficient for reflooding column, $K_c = \left[\frac{\Delta P}{\frac{1}{2}\rho_f v_f}\right]_{\text{core + downcomer}}$
K_l	Loop resistance coefficient, $K_l = \left[\frac{\Delta P}{\frac{1}{2}\rho_g v_g}\right]_{\text{loop}}$
m	Mass
m_e	Mass of liquid slug
$\dot{m}_f$	Core-to-downcomer liquid mass flow rate
$\dot{m}_g$	Rate of vapor generation in core
$\dot{m}_{inj}$	Mass flow rate of coolant injection
$\dot{m}_{out}$	Mass flow rate of vapor out the break
P	Pressure
P_e	Pressure of vapor pocket
P_o	System pressure

P_u	Pressure in upper plenum
Q	Heat transfer rate
R	Gas constant
t	Time
T	Temperature
v	Velocity
V	Vapor volume
V_e	Volume of vapor pocket
V_u	Volume of upper plenum & loop piping
z	Elevation based on bottom of heated length
z_c	Liquid level in core
z_d	Liquid level in downcomer
z_e	Elevation of liquid plug
μ	Dynamic viscosity
ρ	Density
σ	Surface tension

Subscripts

BP	Bottom plenum
c	Core
d	Downcomer
e	Pertaining to the liquid expulsion mechanism
f	Liquid
g	Vapor

l	Loop
sat	Saturation condition
u	Upper plenum & loop
w	wall

1. INTRODUCTION

1.1 LOSS OF COOLANT ACCIDENT

To assure safe operation of nuclear power plants, the Nuclear Regulatory Commission requires the plants to be able to withstand various component and system failures without releasing unacceptable amounts of fission products. One of the possible failures considered is the rupture of a major coolant pipe, leading to a loss of coolant accident (LOCA). The most severe LOCA is postulated to result from a double-ended break in the cold leg of the primary coolant system, since such a break is calculated to lead to the highest hot spot cladding temperatures in the fuel rods.

The phases of a LOCA following the pipe break can be identified as blowdown, refill, and reflood.

Immediately following the rupture, the blowdown phase is a series of severe transients in coolant flow, system pressure, and fuel rod heat transfer. The reactor vessel decompresses rapidly from its operating condition of about 2250 psia (15.5 MPa) to containment pressure, with accompanying loss of coolant. The water coolant flashes to steam as its pressure drops to saturation pressure. A pressure difference between the upper and lower plena builds up in sufficient magnitude to force a stagnation, then reversal, of the core flow. Although the plant protection systems have shut down chain nuclear reactions upon sensing the decompression, radioactive decay of fission products and actinides continue to generate energy at over 5% of the operating power level.

Fueled by this decay energy, the reactor core heats up at a rate of up to 20 °F/sec (11 K/sec), since local and bulk voiding have reduced heat removal from the core.

At about 30 seconds into the LOCA, the blowdown phase is almost complete as the vessel pressure falls to containment pressure and the reactor core is empty of coolant. At different points during blowdown, the various injection components of the emergency core cooling system (ECCS) have been activated by sensing pressure and coolant levels. After the injected coolant has refilled the bottom plenum, it enters and marches up the core, which has by now attained a temperature in excess of 1000 °F (811 K). The fuel rods are initially cooled by film boiling, then by transition and nucleate boiling as the cladding temperature drops below the Leidenfrost temperature. Due to the opposing steam pressure, the reflood rate is limited to about 1 in./sec (2.54 cm/sec).

The LOCA is successfully contained only if the core is completely reflooded before destructive processes, such as rod melting and metal-water reactions, take place.

1.2 REFLOOD DYNAMICS

In a PWR, emergency coolant is injected into the cold leg or downcomer. Gravity pushes the coolant around the bend in the bottom plenum and up the hot channels.

The single most important parameter in reflood analysis is the flooding rate, the net rate at which coolant crosses the inlet of the core. It has been demonstrated in forced-feed, bottom reflood experiments, such as FLECHT [1] , that provided the core flooding rate is high enough, the rod temperatures will stay within safe limits. The flooding rate is determined primarily by two quantities: the downcomer hydraulic head, which drives the flow, and the back pressure in the core, which impedes it. Since vapor generated in the core must vent through paths of consederable resistance, back pressure builds up in the core and limits the flooding rate.

Gravity oscillations are possible during reflood, if driving mechanisms are present. Recently, U-tube type oscillations have been observed in scaled reflood experiments such as FLECHT-SET [2] and SEMISCALE. [3] The frequency of the observed oscillations correlates closely to the natural frequency (about 0.3 Hz) of the systems under test.

The U-tube type oscillations are believed to be generated by the following mechanism. When emergency coolant rushes into the hot core, violent boiling suddenly begins at some point beneath the free surface of the coolant. The high rate of vapor generation creates a pressure pulse which momentarily forces liquid out of the core. After the vapor has vented and the pressure pulse has disappeared, coolant rushes back and the process repeats.

The effects of the oscillations on the flooding rate and core heat removal are not fully understood. The oscillations may enhance core cooling since they increase local fluid velocities and thus local heat transfer coefficients. Reflood tests conducted at the Argonne National Laboratory indicate that such effects are small.[4] However, if the oscillations become too violent, emergency coolant may be thrown out of the reactor core, thus reducing liquid inventory in the core.

1.3 REFLOOD HEAT TRANSFER

Heat transfer from the fuel rods during reflood is a temperature-controlled process. The temperature excursion of the fuel rods can be best explained by a generalized boiling curve shown in Fig. 1.1, which is typically a log-log plot. Since the initial temperature of the fuel rod is high, reflood heat transfer proceeds from the high temperature region to the low temperature region through film boiling, transition boiling, and nucleate boiling.

The key to reflood heat transfer analysis is an accurate knowledge of film boiling heat transfer and minimum film boiling temperature (MFBT), which, being a minimum point on the boiling curve, is an unstable operating condition. At surface temperatures above the MFBT, a vapor film blankets the fuel rod surface so coolant has no direct contact with the surface. Because heat flux is low under such conditions, rod temperature decreases slowly or may even rise if decay heat exceeds surface heat removal.

Once the MFBT is crossed, however, surface heat flux rises rapidly as a result of direct contact between liquid and rod surface, causing surface temperature to drop a few hundred degrees F in a matter of seconds.

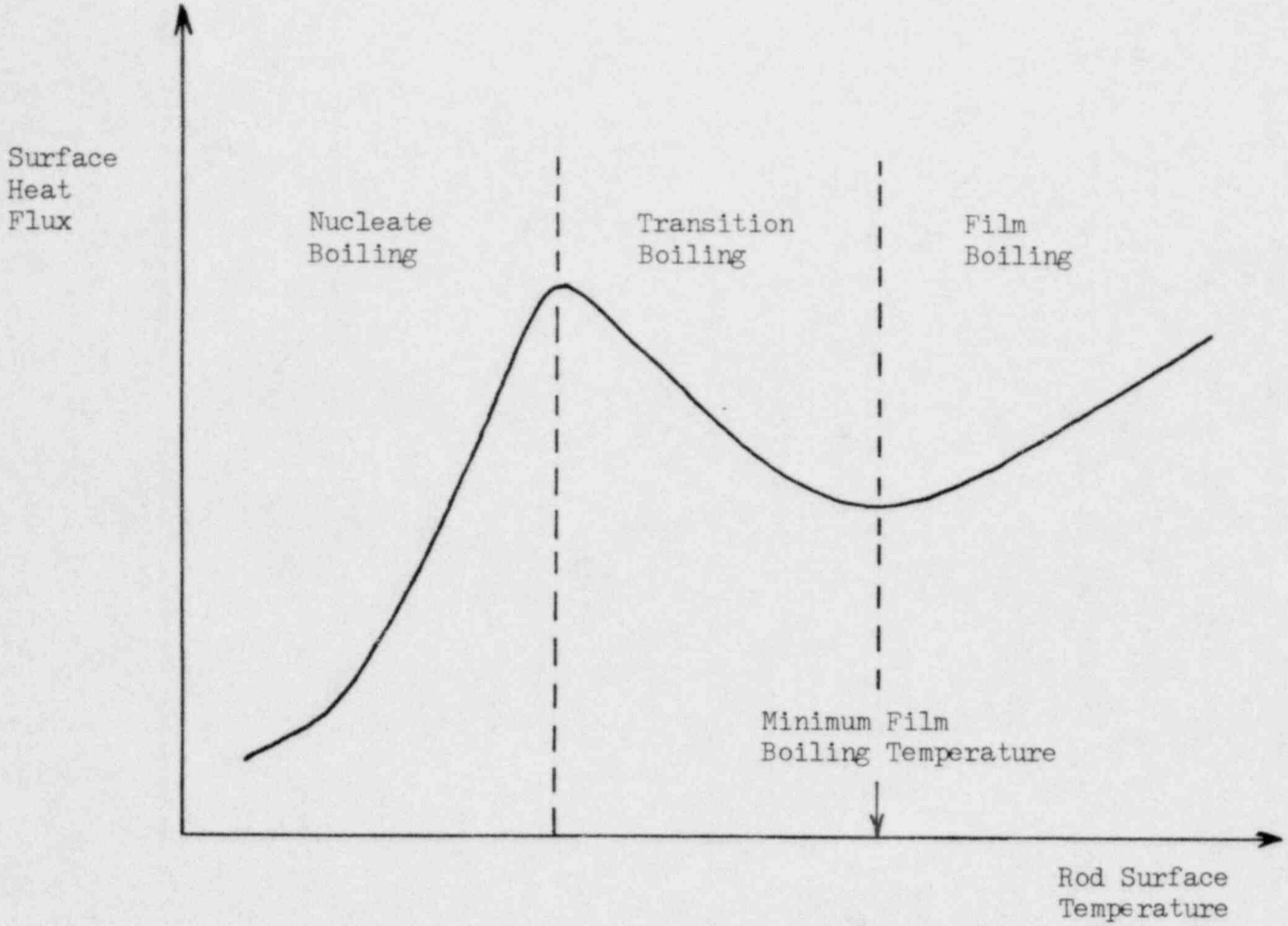

Fig. 1 1 A Generalized Boiling Curve

A good knowledge of two-phase flow patterns along the length of the fuel rods is also essential to reflood heat transfer analysis. Fig. 1.2 shows the flow patterns that can be identified in a vertical channel having an initial temperature higher than the MFBT. Nucleate and transition boiling dominate the inlet region of the channel since surface temperature is lower there. Downstream of the point at which the MFBT is anchored, inverted annular film boiling dominates. In inverted annular film boiling, a superheated vapor film flows around a liquid core. Heat is transferred by convection through the vapor film. Further downstream, the vapor flow rate is so high that the liquid core becomes unstable and breaks up into droplets, which accelerates upwards and out of the channel. In this droplet flow region heat transfer deteriorates significantly since liquid-surface contact is sporadic and contact area is small.

The foregoing description applies only to a steady-state situation, in which case the surface temperature is the important parameter in determining heat flux and flow patterns. During flow and pressure transients, analysis is more difficult because other parameters such as flow velocities and void fractions, which cannot be accurately measured, come into play.

1.4 SCOPE OF STUDY

The purpose of this research is to study the dynamics and heat transfer of coolant flow during the oscillatory phase of bottom reflood

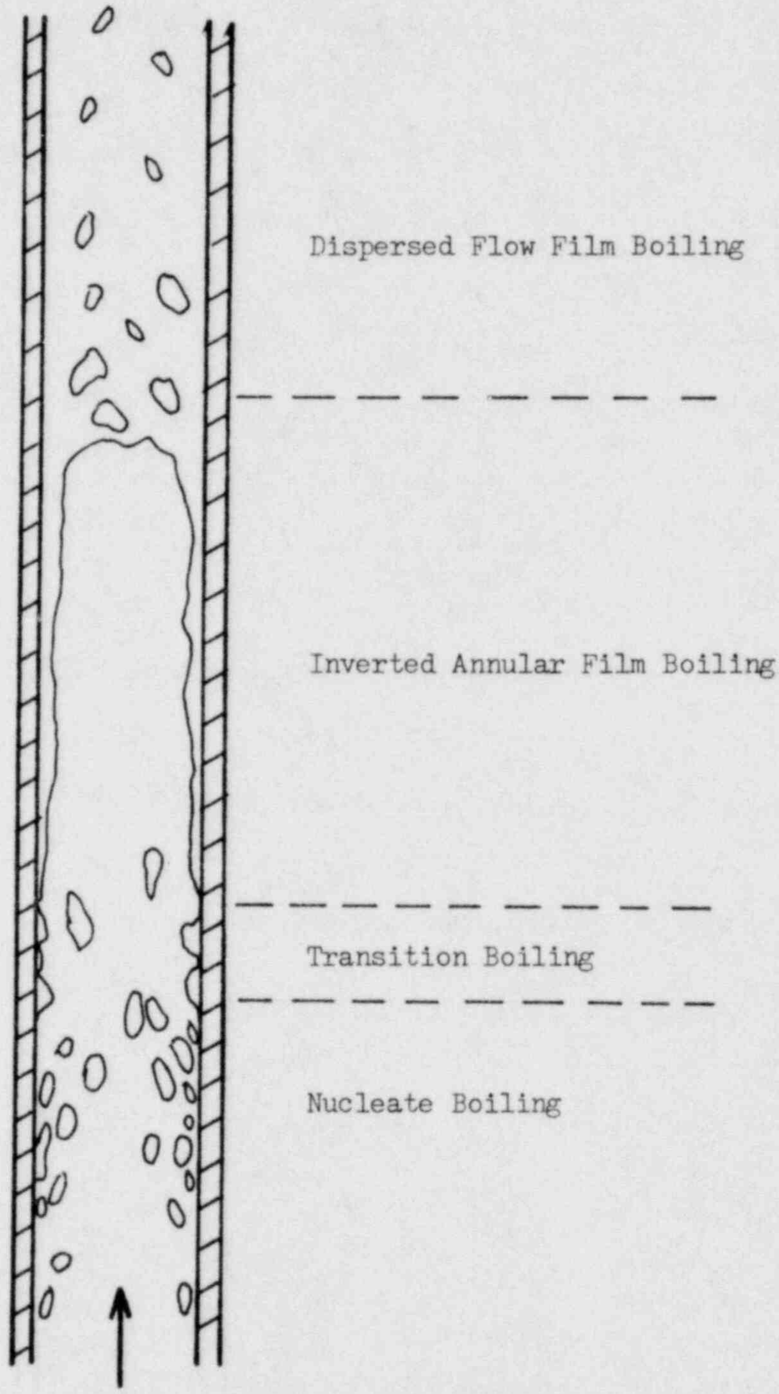

Fig. 1.2 Two-Phase Flow Boiling Regimes in Reflood

and to identify the physical mechanisms responsible for driving and sustaining the oscillations.

A computer model of the reactor system under reflood conditions is developed. The model features single-phase, one-dimensional fluid mechanics with lumped resistance, inertia, and capacitance. Thermodynamic properties are evaluated at system pressure, which is assumed to be constant. Axial conduction in the fuel rods and thermodynamic non-equilibrium between the liquid and vapor phases are ignored. Radial heat transfer coefficients are calculated from a simplified boiling curve in which rod surface temperature is the only dependent variable.

Due to the abundance of published experimental data, no experiments are performed under this research. The FLECHT-SET and Semiscale tests produce reflood data under a wide range of conditions.

From comparisons of the computer model calculations with available experimental results, the assumptions and simplifications in the model are re-examined. The physical phenomena associated with the reflood process, the reflood oscillations in particular, are evaluated and discussed.

2. THEORY

2.1 DRIVING MECHANISM

The large amplitude and sustained nature of the reflood oscillations suggest that a repetitive driving force is at work during reflood. This study proposes a mechanism by which the oscillations can be driven.

Figure 2.1 shows, conceptually, how rod heat flux varies with core elevation. The presence of liquid on the wall makes a difference; therefore we have two cases. In case (a), the liquid level is below the quench front. Since heat flux is low and the liquid is subcooled at the inlet, not very much vapor is being generated. In case (b), the liquid level rises above the quench front, where heat flux is high. If subcooling is removed, rapid vapor generation will begin.

When emergency coolant rushes into the hot core, it overshoots the quench front, where rod heat flux is highest. When the coolant flow stagnates, subcooling is rapidly removed and violent boiling begins at some point beneath the free surface of the liquid. If the rate of vapor generation is so high that the vapor cannot vent fast enough, the liquid trapped above the vapor pocket will be accelerated upwards. Simultaneously, the resulting pressure pulse pushes core coolant downwards. After the vapor has vented, the coolant rushes back up the core and the process repeats.

Figure 2.2 shows a schematic of this coolant flow path for our

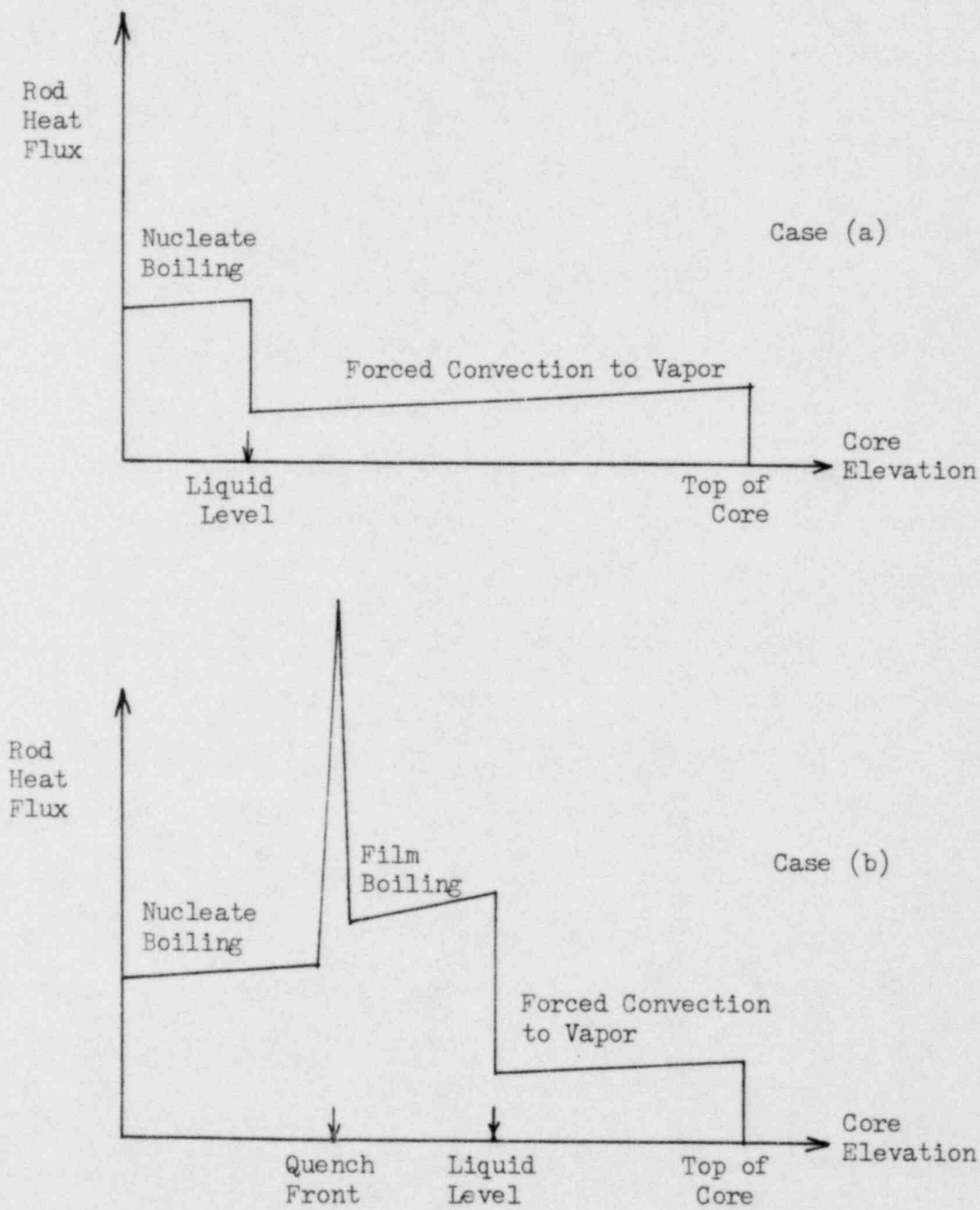

Fig. 2.1 Heat Flux vs. Core Elevation When Liquid Level is (a) Below, (b) Above, Quench Front.

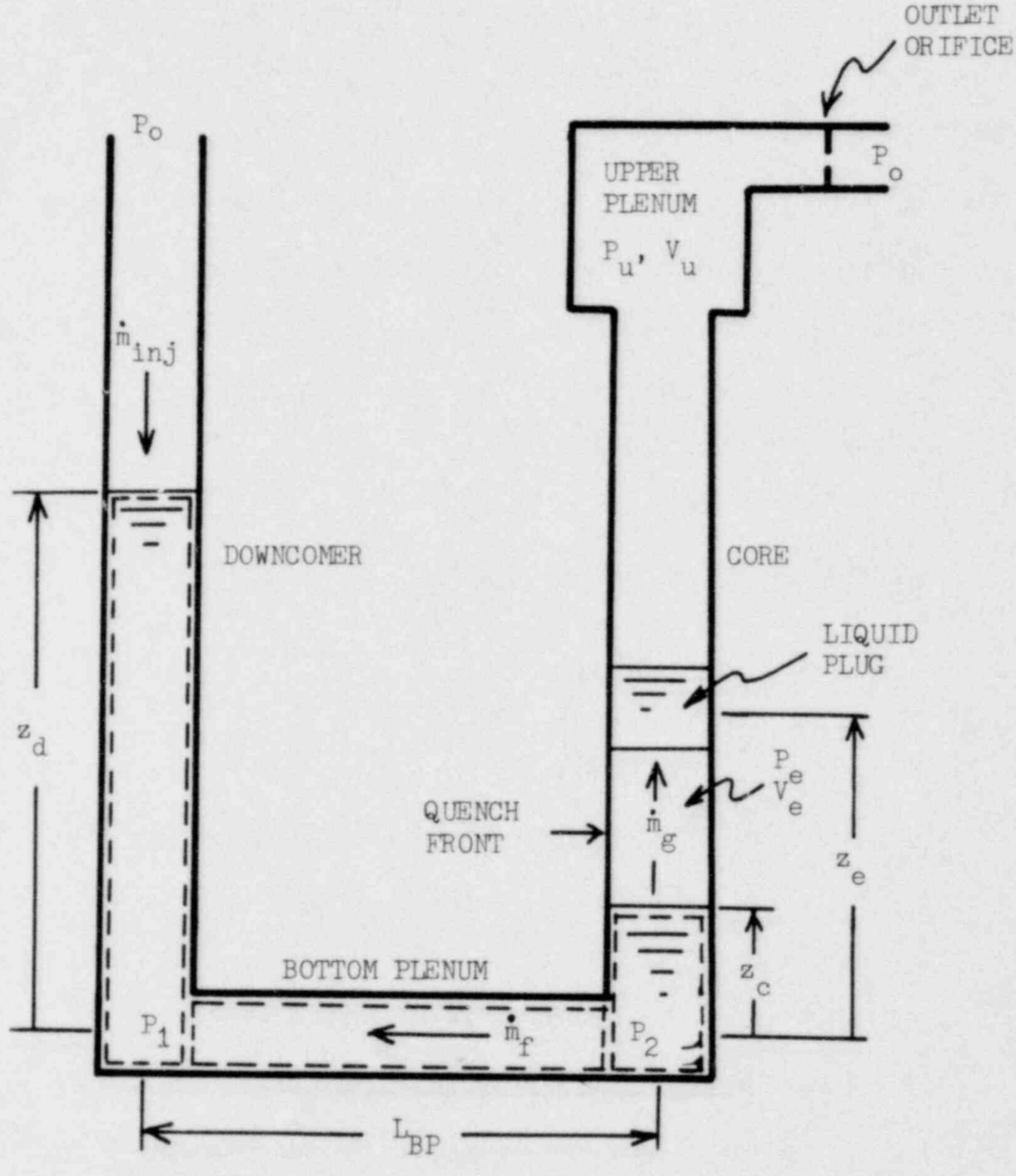

Fig. 2.2 Schematic of Gravity Reflood Model

reflood model. It also shows, at the quench front, the vapor pocket which is expelling liquid above it. In general, some vapor vents through the trapped liquid and exerts a drag force on the liquid. For simplicity, we assume that no vapor vents through so that the trapped liquid acts like a piston. Approximating the pressure P_e of the vapor pocket by the ideal gas law, PV = mRT, one obtains after differentiation and rearrangement:

$$\frac{dP_e}{dt} = \frac{\dot{m}_g RT - P_e A_c (\dot{z}_e - \dot{z}_c)}{A_c (z_e - z_c)} \quad (2.1)$$

A force balance on the liquid plug gives:

$$m_e \ddot{z}_e = (P_e - P_u) A_c - m_e g \quad (2.2)$$

We assume that the liquid slug accelerates upward to its maximum velocity and stays at that velocity until it reaches the upper plenum. It is not allowed to decelerate. Heat transfer to the liquid slug is ignored.

Although the actual mechanism may differ in details from the one described above, some form of liquid expulsion from the core is evident in the reflood experiments. In the single-tube experiment of White and Duffey [5], they noted occassional discharge of large plugs of water from the heated tube. In the FLECHT-SET Phase A tests, sheets of water droplets were observed passing the window at the 9 ft (2.74 m) elevation with a period of about 3 sec.

For simplicity, we have modeled the expelled liquid as a piston. In reality, the expelled liquid is more likely to break up into smaller fractions. Whatever the case may be, the upward acceleration of the expelled liquid must be balanced by a downward acceleration of the continuous reflood column.

The quantitative conditions under which the liquid expulsion occurs are not well understood. The local vapor velocity seems to be the most important parameter. We postulate that liquid expulsion begins when the superficial vapor velocity exceeds a critical value. Lacking better estimates, we will use a critical superficial vapor velocity of 20 ft/s (6.1 m/s) to determine the occurrence of liquid expulsion.

In general, only a fraction of the liquid above the vapor pocket is expelled and carried over to the upper plenum. The other fraction returns to the core due to non-uniform vapor velocities and break-up of the liquid plug. In our calculation we will assume that fraction to be 50%.

2.2 DYNAMICS OF THE CONTINUOUS LIQUID COLUMN

The liquid in the downcomer and core is modeled as a continuous, one-dimensional column of single-phase liquid. The single-phase assumption means that no vapor voids are allowed in the continuous liquid column. All the vapor generated in the core beneath the liquid surface are assumed to rise immediately to the surface. In effect, we assumed an infinite bubble rise velocity but ignore the associated vapor momentum flux. Furthermore, thermal equilibrium and saturation conditions at system pressure are assumed throughout the system.

First, consider this case in which liquid expulsion is not in progress. Then the pressure in the core is approximately equal to that in the upper plenum, P_u. With reference to Fig. 2.2, the force balance on the liquid column in the core is,

$$\rho_f A_c z_c \frac{d(v_f)_c}{dt} = (P_u - P_2)A_c + (\rho_f A_c z_c)g - \tfrac{1}{2}(K_c)_c \rho_f (v_f)_c |(v_f)_c| A_c \tag{2.3}$$

Writing $\dot{m} = \rho A v$ and rearranging:

$$\frac{z_c}{A_c}\frac{d\dot{m}_f}{dt} = (P_u - P_2) + \rho_f z_c g - \frac{(K_c)_c \dot{m}_f |\dot{m}_f|}{2\rho_f A_c^2} \tag{2.4}$$

Similarly for the bottom plenum and downcomer:

$$\frac{L_{BP}}{A_{BP}}\frac{d\dot{m}_f}{dt} = (P_2 - P_1) - \frac{(K_c)_{BP} \dot{m}_f |\dot{m}_f|}{2\rho_f A_{BP}^2} \tag{2.5}$$

$$\frac{z_d}{A_d}\frac{d\dot{m}_f}{dt} = (P_1 - P_o) - \rho_f z_d g - \frac{(K_c)_d \dot{m}_f |\dot{m}_f|}{2\rho_f A_d^2} \tag{2.6}$$

Adding (2.4), (2.5), and (2.6), we get,

$$\left(\frac{z_c}{A_c} + \frac{L_{BP}}{A_{BP}} + \frac{z_d}{A_d}\right)\frac{d\dot{m}_f}{dt} = (P_u - P_o) - \rho_f (z_d - z_c)g - \frac{K_c \dot{m}_f |\dot{m}_f|}{2\rho_f A_c^2} \tag{2.7}$$

Equation (2.7) governs the dynamics of the continuous liquid column. Mass balances give the liquid levels in the downcomer and core:

$$\rho_f A_d \dot{z}_d = \dot{m}_{inj} + \dot{m}_f \tag{2.8}$$

$$\rho_f A_c \dot{z}_c = -\dot{m}_f - \dot{m}_g \tag{2.9}$$

By differentiating and rearranging the ideal gas law, $PV = mRT$, we get for the pressure in the upper plenum:

$$\frac{dP_u}{dt} = \frac{(\dot{m}_g - \dot{m}_{out})RT + P_u A_c \dot{z}_c}{V_u} \tag{2.10}$$

If we ignore vapor acceleration, then the vapor flow rate out the break, $\dot{m}_{out}$, is given by:

$$\dot{m}_{out} = A_l \sqrt{\frac{2\,\rho_g (P_u - P_o)}{K_l}} \tag{2.11}$$

When the liquid expulsion mechanism described in Section 2.1 occurs, two more equations: Eqs. (2.1) and (2.2), are required. Furthermore, the term P_u should be changed to P_e in Eq. (2.7); and $\dot{z}_c$ should be changed to $\dot{z}_e$ in Eq. (2.10).

The rate of coolant injection, $\dot{m}_{inj}$, is a boundary condition. The vapor generation rate, $\dot{m}_g$, is an output from the heat transfer model, which is described in the following section.

2.3 HEAT TRANSFER MODEL

Rod heat transfer provides an important input to the dynamics of the liquid column: the rod heat flux, which yields the vapor generation rate. The complete heat transfer model consists of two parts: a rod conduction model to calculate rod temperature, and a scheme for calculating wall-to-liquid heat flux.

2.3.1 Wall-to-Liquid Heat Transfer

Below the core liquid level, post-CHF heat flux is calculated from Hsu's correlation: [6]

$$h_w = h_{Hsu} + h_{Mod.\ Bromley}$$
$$= 1456\ P^{.558} \exp[-0.003758\ P^{.1733} \Delta T_{sat}]$$
$$+ 0.62 \left[\frac{g k_g^3 \rho_g(\rho_f - \rho_g) H_{fg}}{T_{sat}\, \mu_g} \frac{1}{2\pi} \sqrt{\frac{g(\rho_f - \rho_g)}{\sigma}}\right]^{\frac{1}{4}} \qquad (2.12)$$

Figure 2.3 shows heat flux calculated from the equation plotted against reflood data. Hsu's correlation is chosen because it is based on low void fraction, reflood data. It covers both transition and film boiling and gives heat flux as a function of wall temperature only

Above the core liquid level, heat transfer consists of two components: heat transfer to vapor by forced convection, and heat transfer to entrained liquid droplets by film boiling. Calculation of the droplet component in an unsteady flow is a formidable task by itself. To keep the model simple, we forgo a detailed calculation and allow a

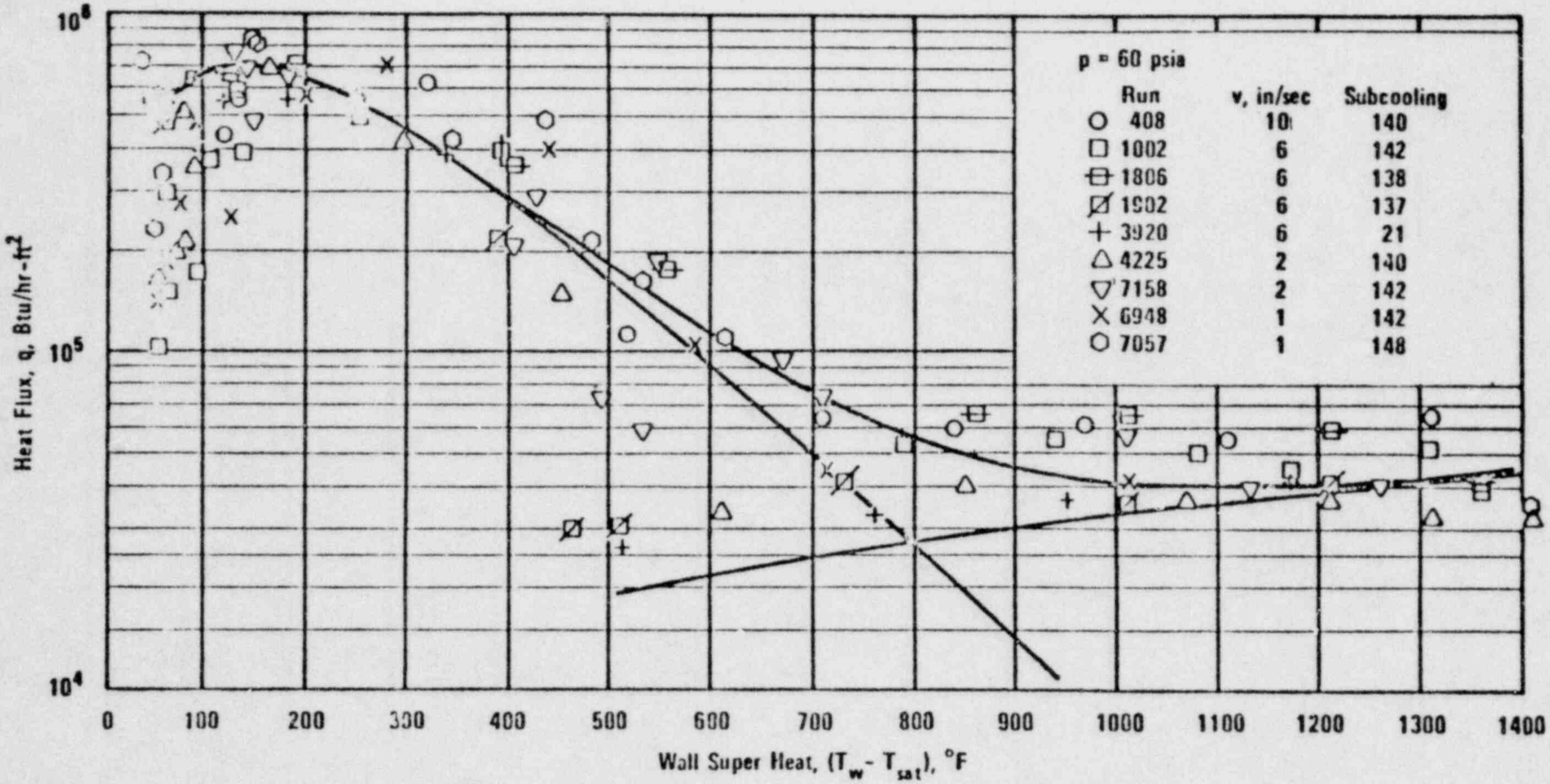

FIG. 2.3 HEAT FLUX AS FUNCTION OF SUPERHEAT FOR TRANSITION AND FILM BOILING AT 60 PSI (Ref. 6)

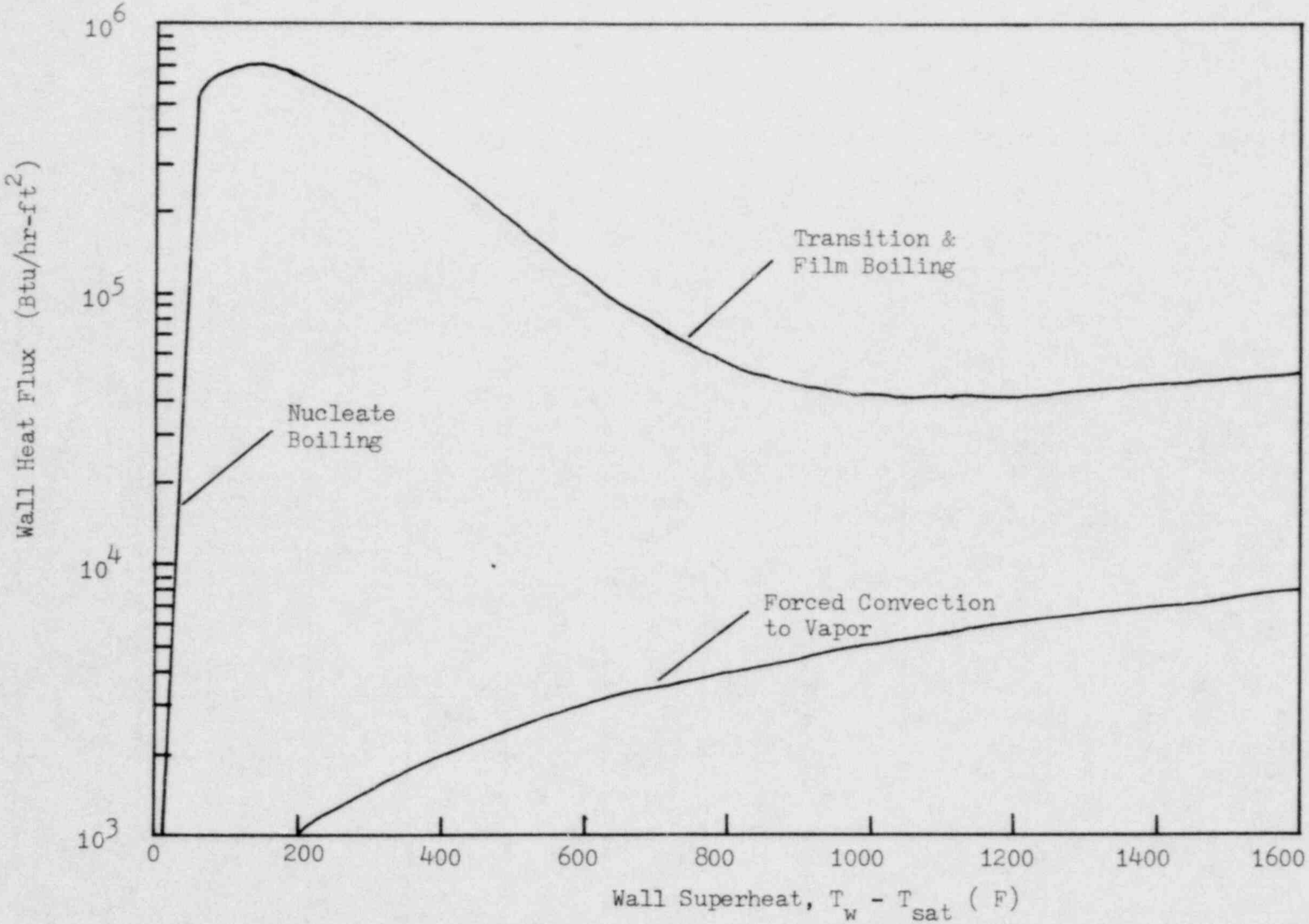

Fig. 2.4 Heat Flux vs. Superheat During Reflood at 60 psi

constant heat transfer coefficient of 5 Btu/hr-ft^2-°F (28.4 W/m^{2}K) for this regime.

After the quench, decay heat is removed by nucleate boiling. However, the selection of nucleate boiling equation is not critical because the low levels of decay heat are always entirely removed by nucleate boiling. McAdam's equation is used here: [6]

$$h_w = 0.074\ (T_w - T_{sat})^{2.86} \tag{2.13}$$

Fig. 2.4 shows heat flux vs. superheat for all three regimes.

2.3.2 Rod Conduction Model

The function of the rod conduction model is to keep track of the rod temperature. It is derived by applying the energy equation to the heater rod:

$$\frac{d}{dt}(\ E_{stored}\ ) = \dot{Q}_{decay} - \dot{Q}_w \tag{2.14}$$

where $$\dot{Q}_w = h_w A_w (\ T_w - T_f\ ) \tag{2.15}$$

While Eq. (2.14) guarantees an overall energy balance for the rod, the accuracy of the transient temperature profile generally depends on the degree of sophistication of the solution technique, which usually entails finite-difference methods. See, for example, the work of Kirchner [7] and Yadigaroglu [8].

For this study, we will use a simple model that is based on two lumped thermal capacities connected by a lumped thermal resistance:

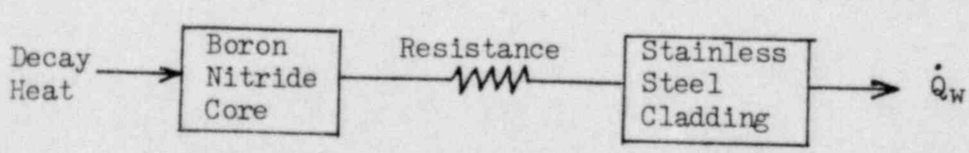

We believe that this second-order model should produce adequate transient response since the cladding is very thin.

2.3.3 Heat Transfer Beyond Core

Heat transfer from bottom quench in the core does not account for all the vapor generation within the primary coolant loop. Some vapor is generated by quenching from the top; some more is generated by evaporation in the upper plenum, loop piping, and steam generators. None of these sources of vapor generation is physically modeled here.

3. RESULTS

3.1 PREDICTION ON EXPERIMENTS

Based on the analytical models presented in Section 2, a computer program is written to obtain numerical solutions. A summary of the analytical models, as well as the initial and boundary conditions for the specfic predictions, are given in Appendix A. Appendix C contains a listing of this computer program.

The hydrodynamic equations in Sections 2.1 and 2.2 are solved with the Runge-Kutta method. Numerical stability requires that a small time step of about 1 millisecond be used. The finite-difference equations of the heat transfer model are implicit so that numerical stability is not a concern. As a compromise between accuracy and computation time, a time step of 0.1 sec and axial nodal size of 0.1 ft are used for the heat transfer model.

Three runs selected from Semiscale Mod-3 [3] and FLECHT-SET Phase A [2] have been calculated. They are FLECHT-SET Run #4923 and Semiscale Tests S-07-4 and S-07-5. The runs conditions are listed in Table 3.1.

Table 3.2 lists the parameters that are specific to the computer calculations. The resistance coefficients K_c and K_l are deduced from information provided by the data reports. The vapor generation rate in the upper plenum, hot leg, and cold leg is an assumed value based on order-of-magnitude estimates. As mentioned in Section 2.3.3, such an effect has not been included in our physical model. However, omission of this effect produces unreasonable results because loop pressure drop, and core and downcomer levels are adversely affected. More meaningful results are obtained if a reasonable rate of vapor generation is allowed in the upper plenum and legs. The parameters pertaining to the driving mechanism are also assumptions. For a detailed list of initial and boundary conditions, refer to Appendix A.

Throughout this report, the term "head" refers to the pressure drop, expressed in liquid height, across a column of liquid. Elevation 0 refers to the bottom of the core heated length. Thus, core head is the pressure drop across the core heated length, from elevation 0 to elevation 3.66 m (12 ft). Downcomer head is the pressure drop, across the downcomer, from elevation 0 to the top of the downcomer.

In the Semiscale tests, core and downcomer heads are measured by differential pressure transducers placed across the core and downcomer. The locations of these pressure transducers are indicated in Fig. 3.1. In FLECHT-SET, the pressure tranducer for the downcomer measures from elevation 0 to the top of the downcomer, the exact elevation of which is not given in the data report.

In Figures 3.2, 3.3, and 3.4, the calculated and measured downcomer and core heads vs. time plots are presented. It should be noted that the quantities compared in these figures are the total liquid heads, or the total pressure drops across the downcomer or core. The pressure drop is the sum of three terms: gravity, acceleration, and friction. During reflood oscillations, the friction term is small, but the acceleration term can be quite large since it responds instantaneously to forces acting on the liquid column. It is the acceleration term that gives rise to the sharp fluctuations observed in the measured and calculated heads. However, the excessively large amplitudes seen in the calculations may be, at least partly, numerical in nature.

Figures 3.5, 3.6, and 3.7 show calculated downcomer heads and calculated downcomer levels for the three runs. The difference between the calculated head and the calculated level represents essentially the calculated acceleration head. It can be seen that the level oscillations are much smoother than the head oscillations. Thus it can be deduced that the sharp pulses in the head oscillations arise from the acceleration term. In fact, the level is equal to the liquid acceleration, which produces the acceleration head, integrated twice with respect to time.

Figure 3.8 shows the calculated vapor velocity at the core exit vs. time for FLECHT-SET Run #4923, which is representative of the other two Semiscale runs. The exit vapor velocity periodically falls below the flooding velocity, which is about 30 ft/s (9.1 m/s) at 40 psia (276 kPa). During these low velocity periods the carryover liquid in the upper plenum should be able to drain into the core.

Table 3.1 Initial Conditions for Selected Runs

	FLECHT-SET #4923	Semiscale S-07-4	Semiscale S-07-5
System Pressure (kPa)	421	421	127
Peak Power (kW/m)	2.3	2.1	1.3
Peak Clad Temperature (K)	873	800	960
ECCS Injection:			
Coolant Temperature (K)	343	334	350
High Rate (kg/s)	4.78	1.22	1.16
Low Rate (kg/s)	0.54	0.10	0.15
Duration of High Rate (s)	14	16	12

Table 3.2 Parameters in Computer Simulation

	FLECHT-SET #4923	Semiscale S-07-4	Semiscale S-07-5
Core Resistance Coefficient, K_c	11	15	15
Loop Resistance Coefficient, K_l	31	400	400
Vapor Generation Rate in Upper Plenum + Both Legs (kg/s)	0.14	0.05	0.02
Driving Mechanism:			
Critical Vapor Velocity (m/s)	6.1	6.1	6.1
Fraction of Liquid Expelled	0.5	0.5	0.5

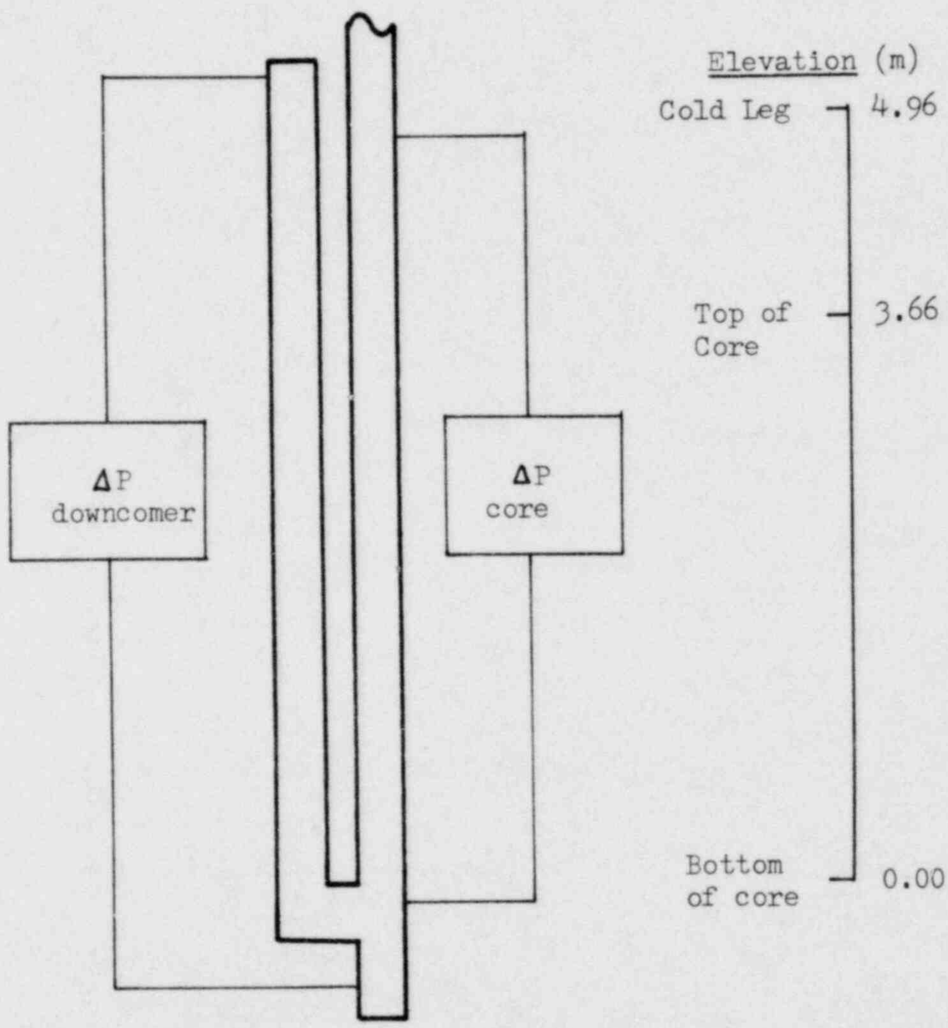

Fig. 3.1 Location of Differential Pressure Transducers for Semiscale Tests

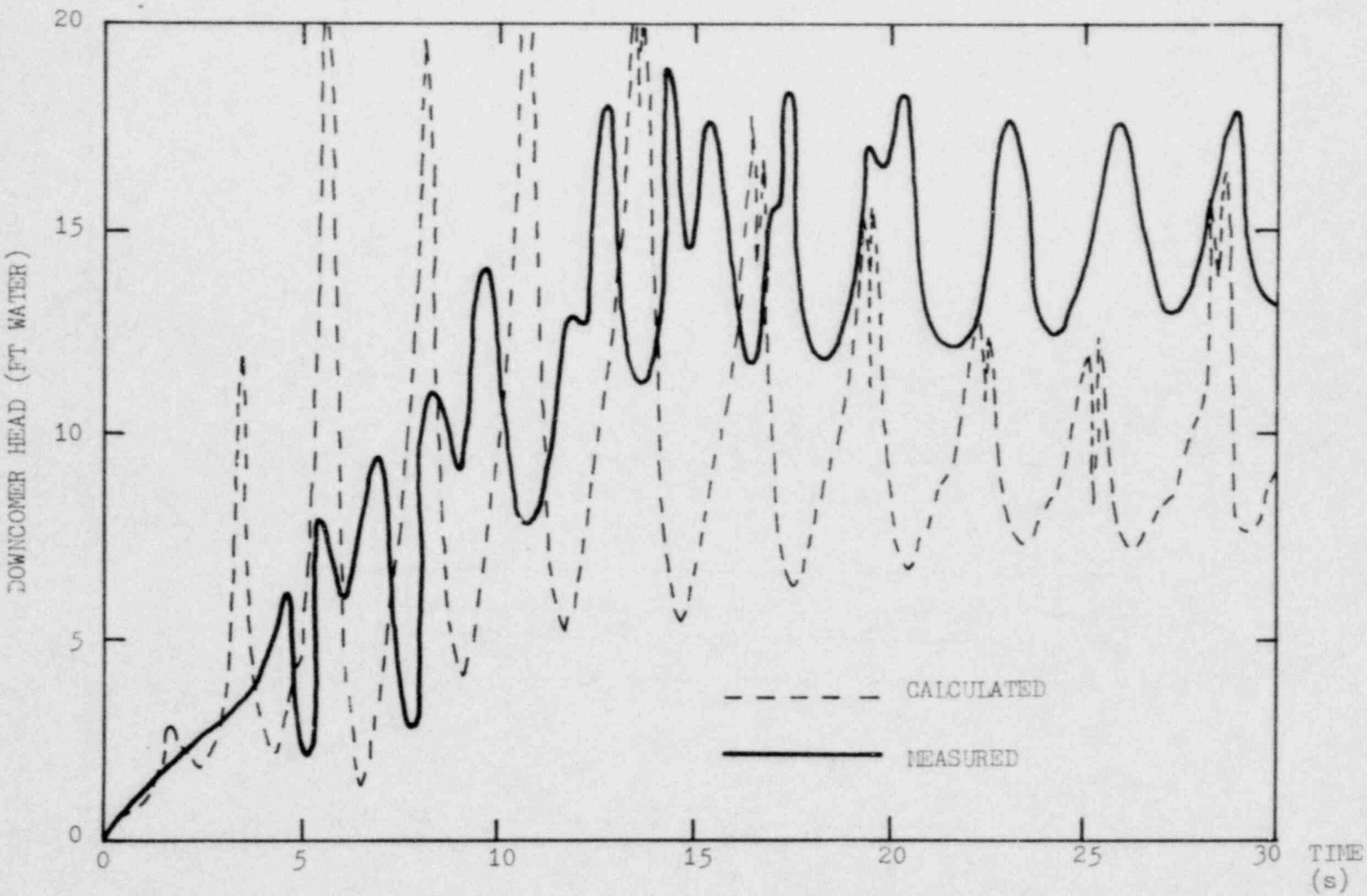

Fig. 3.2 Measured and Calculated Downcomer Head for FLECHT-SET Run #4923 (61 psia)
Initial Clad Temp.: 1111 F, Peak Power: 0.7 kW/ft, Injection Temp.: 158 F
Injection Flow Rate: 10.52 lb/s First 14 s, 1.19 lb/s thereafter

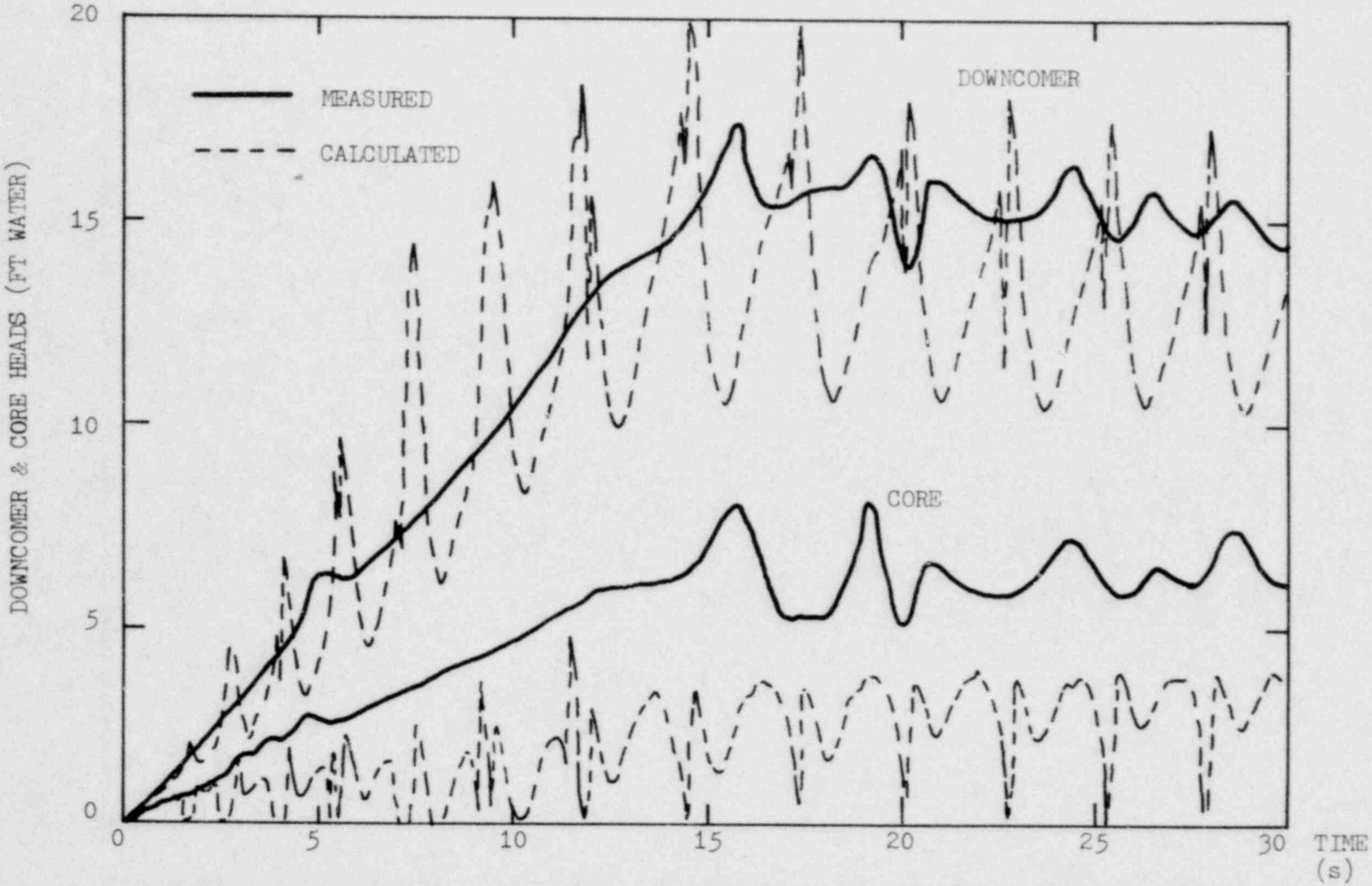

Fig. 3.3 Measured and Calculated Downcomer and Core Heads for Semiscale Test S-07-4 (60 psia)
Initial Clad Temp.: 980 F, Peak Power: 0.63 kW/ft, Injection Temp.: 141 F
Injection Flow Rate: 2.69 lb/s First 16 s, 0.21 lb/s thereafter

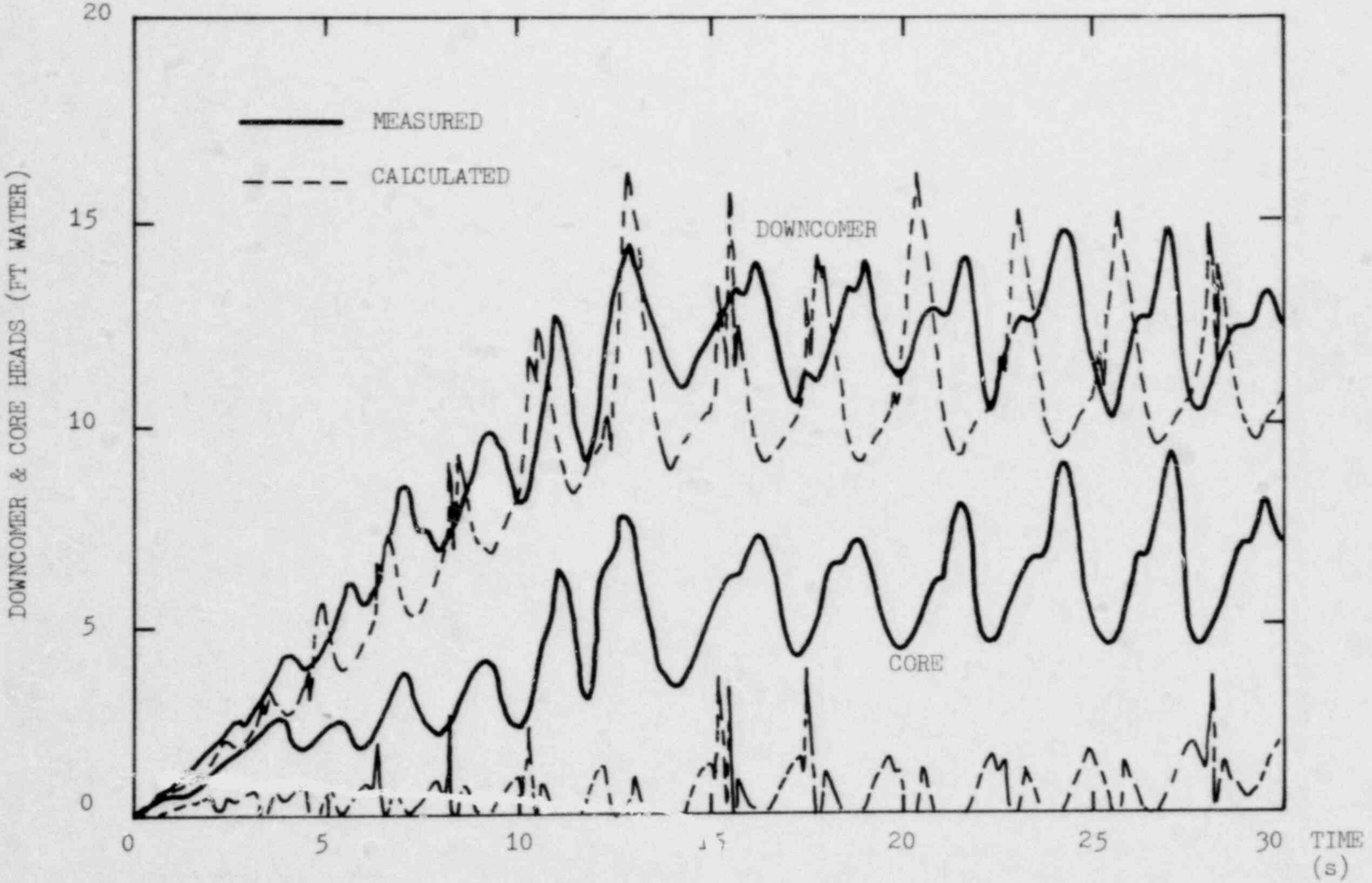

Fig.3.4 Measured and Calculated Downcomer and Core Heads for Semiscale Test S-07-5 (18.4 psia)
Initial Clad Temp.: 1268 F, Peak Power: 0.405 kW/ft, Injection Temp.: 170 F
Injection Flow Rate: 2.55 lb/s First 12 s, 0.34 lb/s thereafter

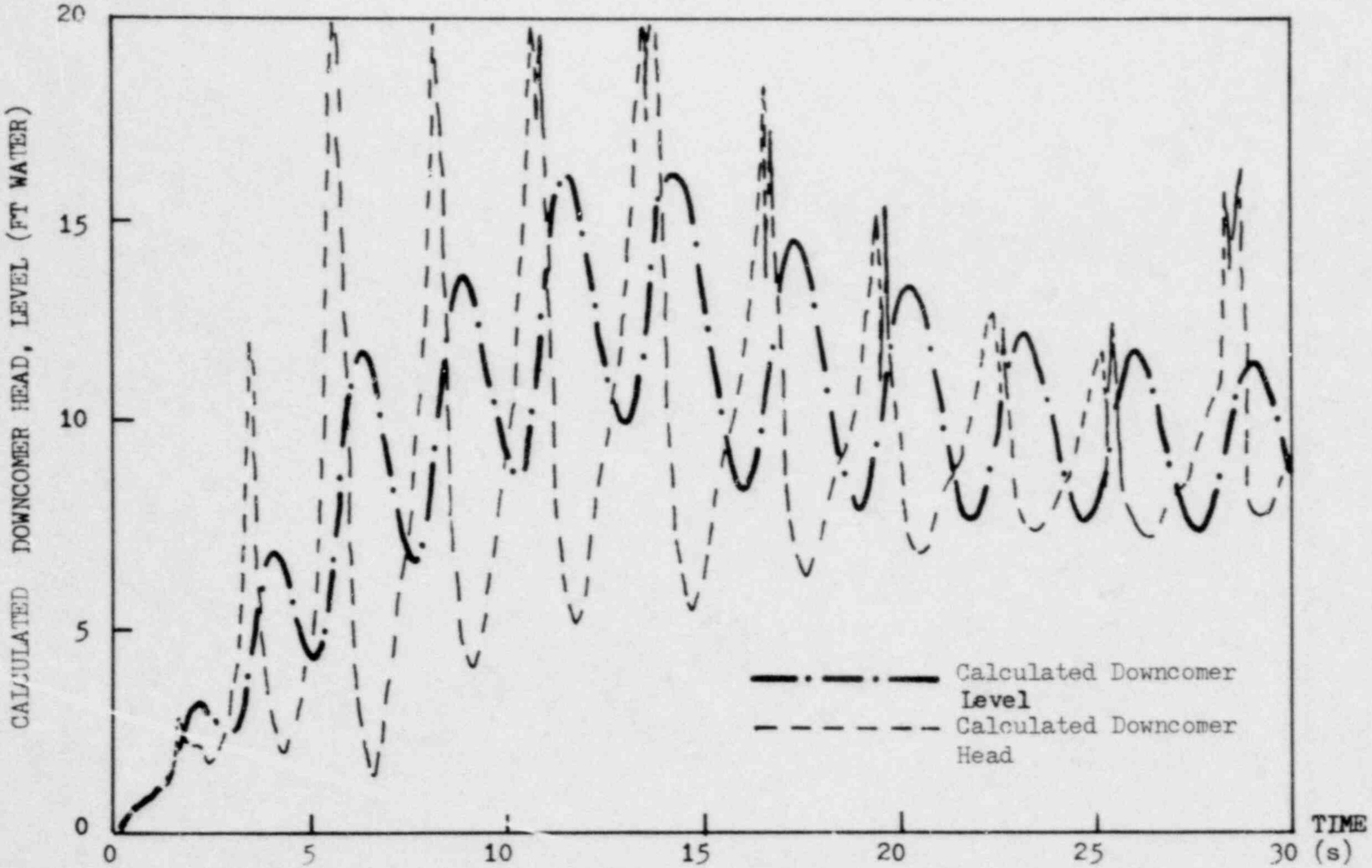

Fig. 3.5 Calculated Downcomer Head & Calculated Downcomer Level for FLECHT-SET Run #4923

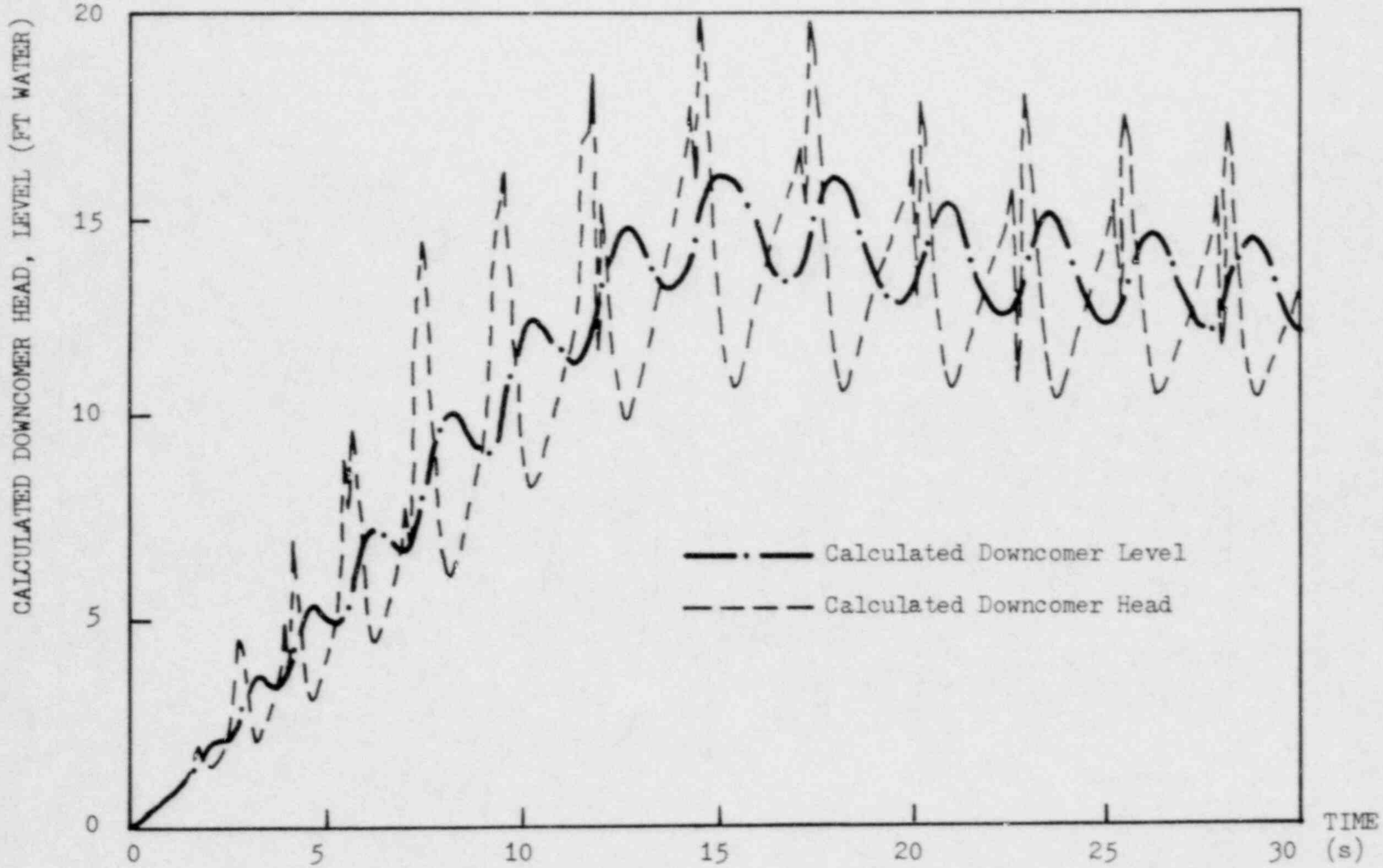

Fig. 3.6 Calculated Downcomer Head & Calculated Downcomer Level for Semiscale Test S-07-4

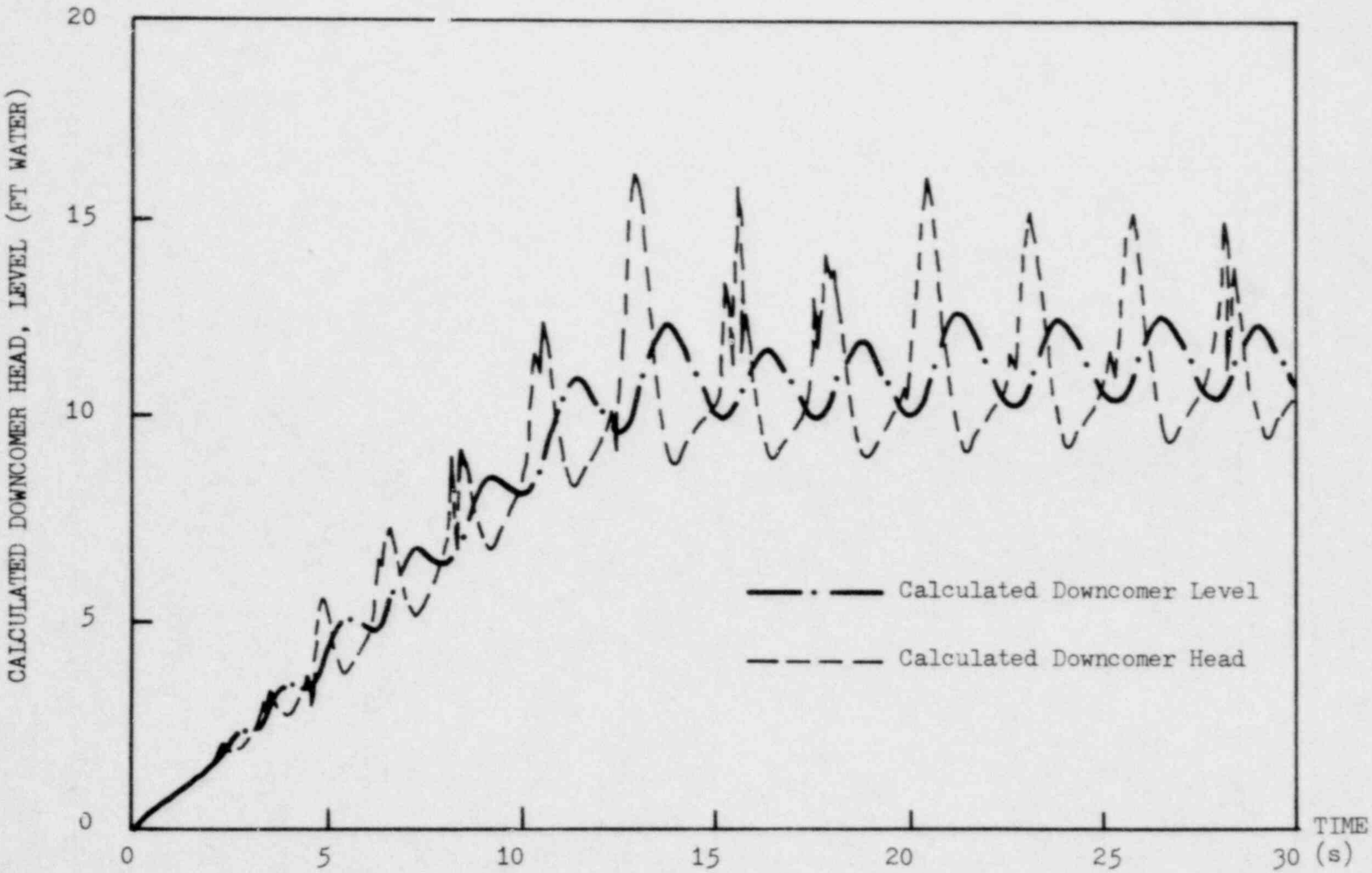

Fig. 3.7 Calculated Downcomer Head & Calculated Downcomer Level for Semiscale Test S-07-5

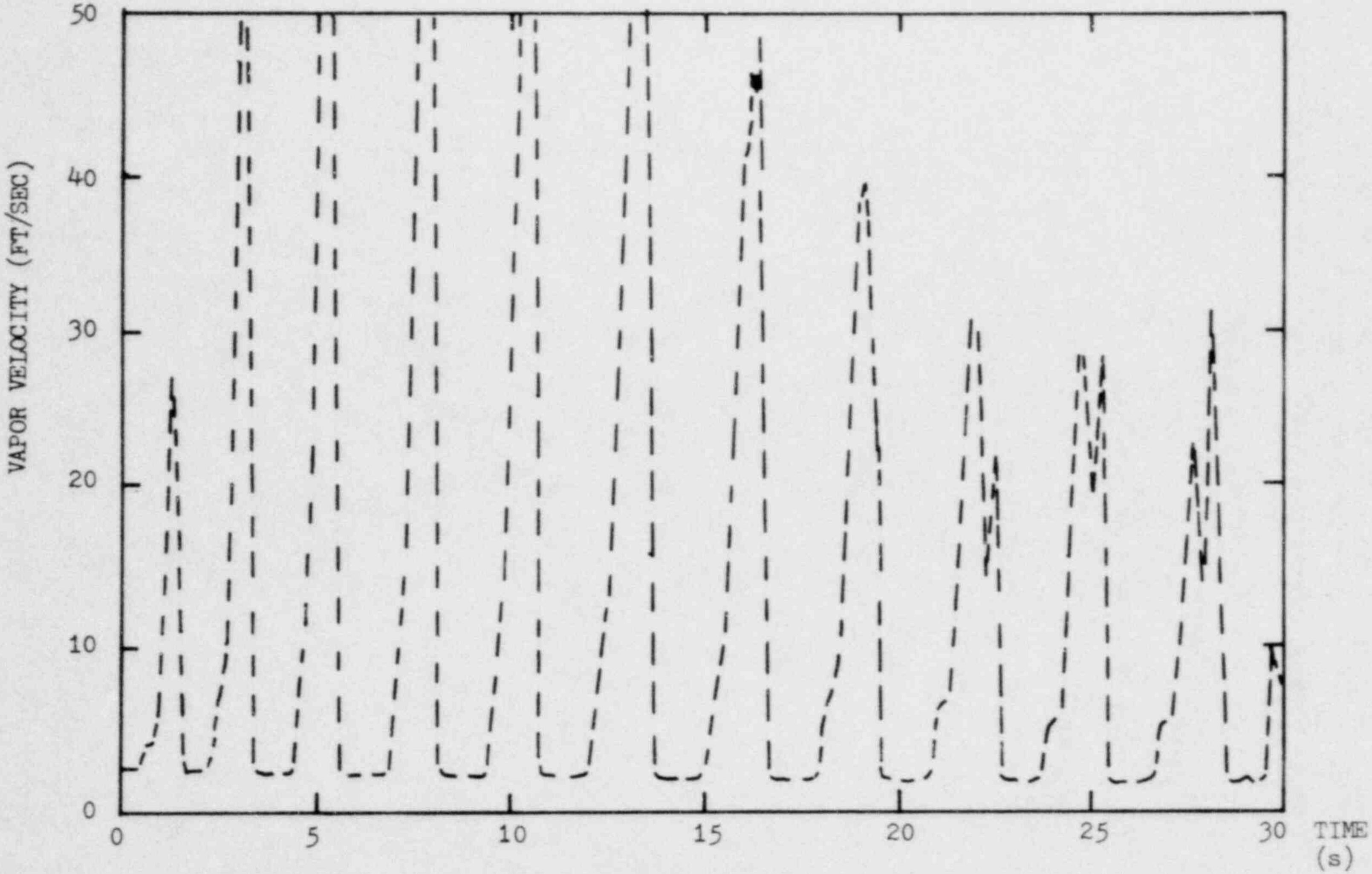

Fig. 3.8 Calculated Vapor Velocity at Core Exit for FLECHT-SET Run #4923

3.2 DISCUSSIONS & RECOMMENDATIONS

3.2.1 Driving Mechanism

The calculations show that the proposed driving mechanism can indeed start and sustain coolant oscillations during reflood. However, the quantitative conditions under which the liquid expulsion mechanism occurs are not well understood. What is the minimum vapor generation that can cause liquid expulsion? What fraction of the liquid trapped above the vapor pocket is expelled and carried into the upper plenum? The answers to these questions affect intimately the dynamics of the reflood oscillations. It should be worthwhile to perform a single-tube experiment with observing and analyzing such a mechanism in mind.

3.2.2 Frequency and Amplitude

While the frequencies of the calculated oscillations agree quite well with data, the amplitudes do not agree as well. The amplitudes depend on the magnitude and duration of the driving force, which in turn depend on the mass of liquid expelled and the history of vapor generation during a quench. The mass of liquid expelled is sensitive to the assumptions of the driving mechanism. The history of the vapor generation rate during a quench is sensitive to the slope of the boiling curve in transition boiling, and to the nodal and time step size of the numerical solution.

3.2.3 Vapor Generation Beyond Core

In the scaled experiments, the thermal capacity of the metal in the upper plenum and loop piping is large so that a significant amount of vapor will be generated if the metal temperature is above the saturation temperature of the fluid. Moreover, fluctuating vapor flow rates may give rise to condensation and evaporation cycles. When vapor flow rate increases, so do the pressure and the saturation temperature. Some vapor condenses, heating up the metal. When vapor flow rate decreases, the pressure falls so that the stored vapor and carry-over liquid become superheated. Evaporation then takes place.

We believe that the above interactions are peculiar to the scaled experiments due to the large ratio of metal surface area to flow volume in those experiments. In full-scale reactor, the effects of such interactions will be much less, since the area/volume ratio is much smaller.

3.2.4 Prediction on Core Head

By making an assumption on the amount of vapor generated in the upper plenum and loop piping, we have been able to increase the loop pressure drop and raise the downcomer liquid head to match the data more closely. However, the calculated core liquid head is low due to two reasons. First, in the experiments, core head is measured from the bottom plenum to the top of the upper plenum. The measurements thus include the head of liquid stored in the upper plenum. Second, the driving mechanism may be expelling too much liquid from the core, thereby reducing both downcomer and core heads.

3.2.5 Draining of Carryover Liquid

The calculated vapor velocity at core exit fluctuates widely. It periodically falls way below the flooding velocity, which is about 30 ft/sec (9.1 m/s) at 40 psia (276 kPa). During these low velocity periods the carryover liquid in the upper plenum should be able to drain into the core.

3.2.6 Single-Phase Assumption

The single-phase assumption on the core liquid works out quite well. It allows lumping of the fluid mechanics, thus avoiding a full-blown finite-difference solution.

Core heat transfer is probably underestimated. In reality, the liquid column swells due to void formation, thus providing more area for heat transfer. Conceivably, one can retain the single-phase assumption in modeling the dynamics of the liquid column, and calculate the swollen liquid level with a quasi-steady void model.

3.2.7 Liquid Level vs. Liquid Head

Care should be taken when one interprets the data on differential pressure, or liquid head, across the core and downcomer. Liquid level and liquid head are equivalent only in a static situation.

In a dynamic situation, liquid head is the sum of three components: the gravity, friction, and acceleration heads. The gravity head is equal to the liquid level in a single-phase liquid, or to the "collapsed" liquid level in a liquid/vapor two-phase system. During reflood oscillations, the friction head is quite small, but the acceleration head is comparable in magnitude to the fluctuation in the gravity head.

Figures 3.5, 3.6, and 3.7 show the calculated downcomer heads and calculated downcomer levels. The difference between the two quantities is significant.

4. CONCLUSIONS

1. The proposed driving mechanism initiates and sustains oscillations during reflood. However, the details of the mechanism are not well understood, and should be investigated.
2. The calculations show that the vapor velocity at the core exit should exhibit cyclical variations. When the vapor velocity is low, carryover liquid that is stored in the upper plenum should be able to drain back into the core.
3. In the scaled experiments, the loop piping provides large metal surface areas on which evaporation and condensation may take place. These interactions are not expected to be significant in a full-scale reactor.

REFERENCES

1. Westinghouse Electric Corporation, FLECHT Reports WCAP-7435, 7444,7544,7665,7931,8651,8838, Westinghouse Electric Corporation, 1970-1978.

2. J.A. Blaisdell et al, "PWR FLECHT-SET Phase A Report," WCAP-8238, Westinghouse Electric Corp., Dec. 1973.

3. R. L. Gillins et al, "Experimental Data Reports for Semiscale Mod-3 Reflood Heat Transfer Test S-07-4," NUREG/CR-0254, TREE-1224, Aug. 1978.

4. Argonne National Laboratory, "Light-Water-Reactor Safety Research Program: Quarterly Progress Report," NUREG/CR-0828, ANL 79-18, pp. 12-18, April 1979.

5. E.P. White and R.B. Duffey, "A Study of the Unsteady Flow and Heat Transfer in the Reflooding of Water Reactor Cores," Annals of Nuclear Energy, Vol. 3, pp. 197-210, 1976.

6. Y.Y. Hsu, "Proposed Heat Transfer 'Best Estimate' Packages," draft, USNRC, Nov. 1977.

7. W.L. Kirchner and P. Griffith, "Reflood Heat Transfer in a Light Water Reactor," NUREG-0106, NRC-24, 1976.

8. G. Yadigaroglu and L. Arrieta, "Analytical Model for Bottom Reflooding Heat Transfer in Light Water Reactors (The UCFLOOD Code)," EPRI NP-756, Project 248-1, Key Phase Report, Aug. 1978.

9. Y.L. Cheung and P. Griffith, "A Revision of Post-CHF Heat Transfer for the REFLUX Code," a report prepared for USNRC, April 1978.

Appendix A. SUMMARY OF ANALYTICAL MODEL

A.1 HYDRODYNAMIC EQUATIONS

The assumptions are:

1. One-dimensional, uniform, single-channel flow for core and downcomer.
2. Single-phase liquid along continuous liquid column, in which void fraction is either 0 or 1.
3. Liquid expulsion starts when the cumulative vapor generation rate below a core elevation exceeds a critical value; 50% of the liquid above that elevation is then expelled. Expelled liquid behaves as a piston.

Equations for the "unforced" dynamics are:

$$\left(\frac{z_c}{A_c} + \frac{L_{BP}}{A_{BP}} + \frac{z_d}{A_d}\right) \frac{d\dot{m}_f}{dt} = (P_u - P_o) - \rho_f(z_d - z_c)g - \frac{K_c \dot{m}_f |\dot{m}_f|}{2\rho_f A_c^2} \quad (A.1)$$

$$\rho_f A_d z_d = \dot{m}_{inj} + \dot{m}_f \quad (A.2)$$

$$\rho_f A_c z_c = - \dot{m}_f - \dot{m}_g \quad (A.3)$$

$$\frac{dP_u}{dt} = \frac{(\dot{m}_g - \dot{m}_{out})RT + P_u A_c \dot{z}_c}{V_u} \quad (A.4)$$

$$\dot{m}_{out} = A_l \sqrt{\frac{2\rho_g (P_u - P_o)}{K_l}} \quad (A.5)$$

Liquid expulsion occurs at $z = z_c$ in the core when

$$j_g(z_e) > (j_g)_{crit} \quad (A.6)$$

where $\quad j_g(z_e) = \int_{z=0}^{z=z_e} \frac{d\dot{m}_g}{\rho_g A_c}$ (A.7)

and $\quad (j_g)_{crit} = 20$ ft/s (6.1 m/s) (A.8)

Mass of liquid expelled or "carried over" is 50% of the liquid above z_e:

$$m_e = \tfrac{1}{2}\rho_f A_c(z_c - z_e) \tag{A.9}$$

Pressure of the vapor pocket is

$$\frac{dP_e}{dt} = \frac{\dot{m}_g RT - P_e A_c(\dot{z}_e - \dot{z}_c)}{A_c(z_e - z_c)} \tag{A.10}$$

Equation of motion of the liquid plug:

$$m_e \ddot{z}_e = (P_e - P_u)A_c - m_e g \tag{A.11}$$

A.2 HEAT TRANSFER PACKAGE

Below continuous liquid level ($z < z_c$), heat transfer coefficient is determined by rod temperature T_w:

$T_w > T_{CHF}$:

$$h_w = h_{Hsu} + h_{Mod.\ Bromley} \quad \text{(Eq. 2.12)} \tag{A.12}$$

$T_{Boil} < T_w < T_{CHF}$:

$$h_w = 0.074(T_w - T_{sat})^{2.86} \tag{A.13}$$

$T_w < T_{Boil}$:

$$h_w = 0.023\,\frac{k_f}{D}\,Re^{0.8}Pr^{0.4} \tag{A.14}$$

T_{CHF} and T_{Boil} (incipience of boiling) are determined from the intersection of the three equations. In Eq. (A.14), the Reyrolds number Re and Prandtl number Pr are based on a constant liquid velocity of 1 in/s (2.54 cm/s) and saturated liquid conditions.

A.3 INITIAL & BOUNDARY CONDITIONS

Initial conditions used in the calculations are derived from the experimental run conditions, Table 3.1. Initial vapor flow rate is assumed to be zero. Initial rod temperatures are interpolated from a truncated sine curve fit to initial rod temperature data:

$$0 < z < z_p: \qquad T_w(z) = T_w(0) + \left[\frac{T_w(z_p) - T_w(0)}{z_p}\right] z$$

$z_p < z < z_m$:

$$T_w(z) = T_w(z_p) + \left[T_w(z_m) - T_w(z_p)\right] \sin \frac{\pi(z - z_p)}{2(z_m - z_p)} \qquad (A.15)$$

where z_m is the mid-plane elevation and z_p is the intersection of the linear and sine curve fit. The function is symmetrical about $z = z_m$.

Boundary conditions are less well-defined than initial conditions. Coolant temperature at core inlet is determined from test data, using a bottom plenum fluid temperature that is closest to the core inlet. Two linear segments with slopes s_1, s_2, are then fitted to the data:

$$t < t_1: \qquad T_{in} = T_1 + s_1 t$$

$$t > t_1: \qquad T_{in} = T_2 + s_2(t - t_1) \qquad (A.16)$$

The amount of steam generated beyond the core, $\dot{m}_v$, is given by:

$$t < 10s \qquad \dot{m}_v = \dot{m}_{vo} t/10$$

$$t > 10s \qquad \dot{m}_v = \dot{m}_{vo} \qquad (A.17)$$

Injection flow rates are given in Table 3.1. Decay heat is calculated from a curve fit to the ANS+20% curve. Table A.1 gives the values of the parameters in Eqs. (A.15), (A.16), (A.17).

Table A.1 Parameters for Initial & Boundary Conditions

	FLECHT-SET #4923	Semiscale S-07-4	Semiscale S-07-5
Truncated sine curve fit to initial wall temperatures:			
$T_w(0)$ (K)	533.3	420	350
$T_w(z_p)$ (K)	644.4	460	740
$T_w(z_m)$ (K)	866.7	800	960
z_p (m)	0.61	0.15	0.7
Linear fit to inlet coolant temperature:			
T_1 (K)	358.3	366.7	350
T_2 (K)	369.4	338.9	350
s_1 (K/s)	1.11	-1.39	0
s_2 (K/s)	-0.25	0	0
t_1 (s)	10	20	50
Vapor generation rate beyond core, $\dot{m}_{vo}$ (kg/s)	0.136	0.046	0.023

Appendix B. REFLUX2 CALCULATION C... RCED OSCILLATORY REFLOOD TESTS

Argonne National Laboratory (ANL) has run single-tube reflood tests by forcing an oscillatory flow into the preheated tube. (For details of the tests, refer to reference [4].) Quench times for various oscillatory frequencies do not differ significantly, suggesting that steady-state heat transfer correlations can be applied to oscillatory reflood conditions.

Three ANL runs have been calculated with the REFLUX2 code [9], a modified version of the REFLUX code [7]. The calculations were made before the experimental results were available. The experimental run conditions are listed in Table B.1. The initial tube wall temperature varies almost linearly from 1000 °F (811 K) at the inlet to 1250 °F (950 K) at the 10 ft (3.05 m) elevation. The inlet velocity function used in the calculations is shown in Figure B.1. Figure B.2 shows the comparison on quench times. Figure B.3 shows temperature vs. time at the 3 ft (0.91 m) and 6 ft (1.83 m) elevations for Run #33.

The most striking discrepancy between the calculated and experimental quench times is that in the experiments, the entrance region of the heated section quenches much earlier. Part of this discrepancy can be attributed to the lack of details in the initial temperature distribution used in the calculations. Other than that, the early quench of the entrance region in the experiments would indicate a high value for the effective heat transfer coefficient. REFLUX2, however, predicts film boiling since the initial wall temperature is about 1000 °F (811 K) and calculates a much lower heat transfer coefficient. REFLUX2 also ignores axial conduction in the tube wall.

The agreement between measured and calculated values is good, considering the various uncertainties of the heat transfer calculation in REFLUX2. Since REFLUX2 uses steady-state heat transfer correlations, the comparisons would suggest that such correlations are valid under oscillatory flow.

Table B.1 Run Conditions for ANL Reflood Tests

	Run #32	Run #33	Run #36
Frequency of inlet flow oscillations (Hz)	0.95	2.94	0
Coolant inlet temperature (K)	338	338	338
Average inlet velocity (cm/s)	20.6	21.1	20.8
Average inlet velocity during forward flow (cm/s)	46.1	47.1	20.8
Average inlet velocity during reverse flow (cm/s)	5.0	4.9	0

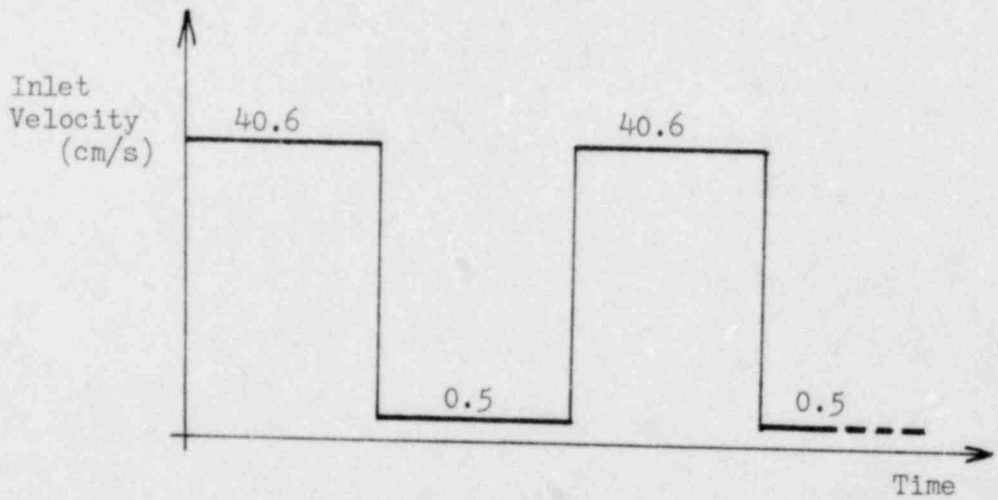

Fig. B.1 Inlet Velocity Function Used in Calculating ANL Tests

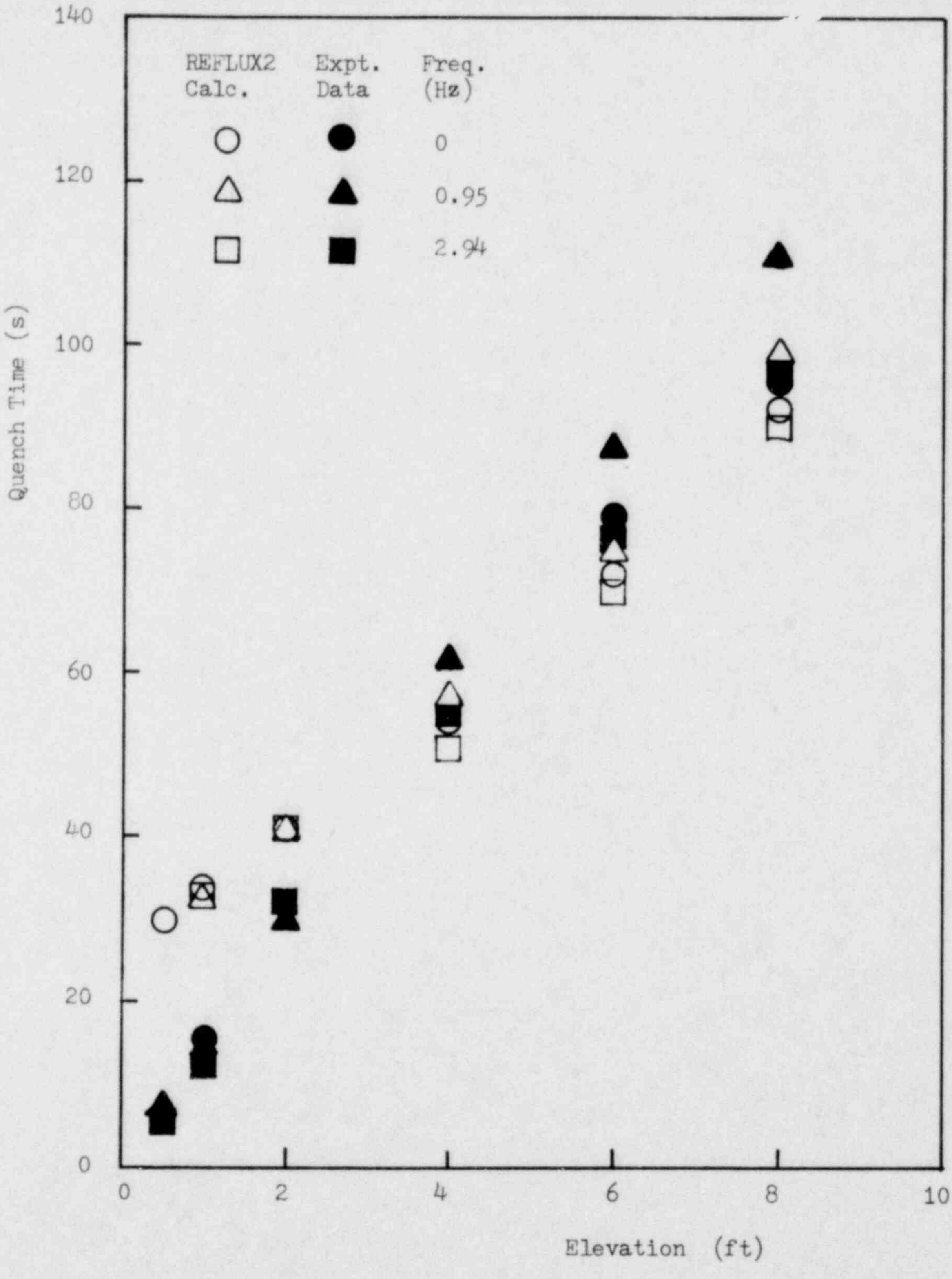

Fig. B.2 Measured and Calculated Quench Times for ANL Tests

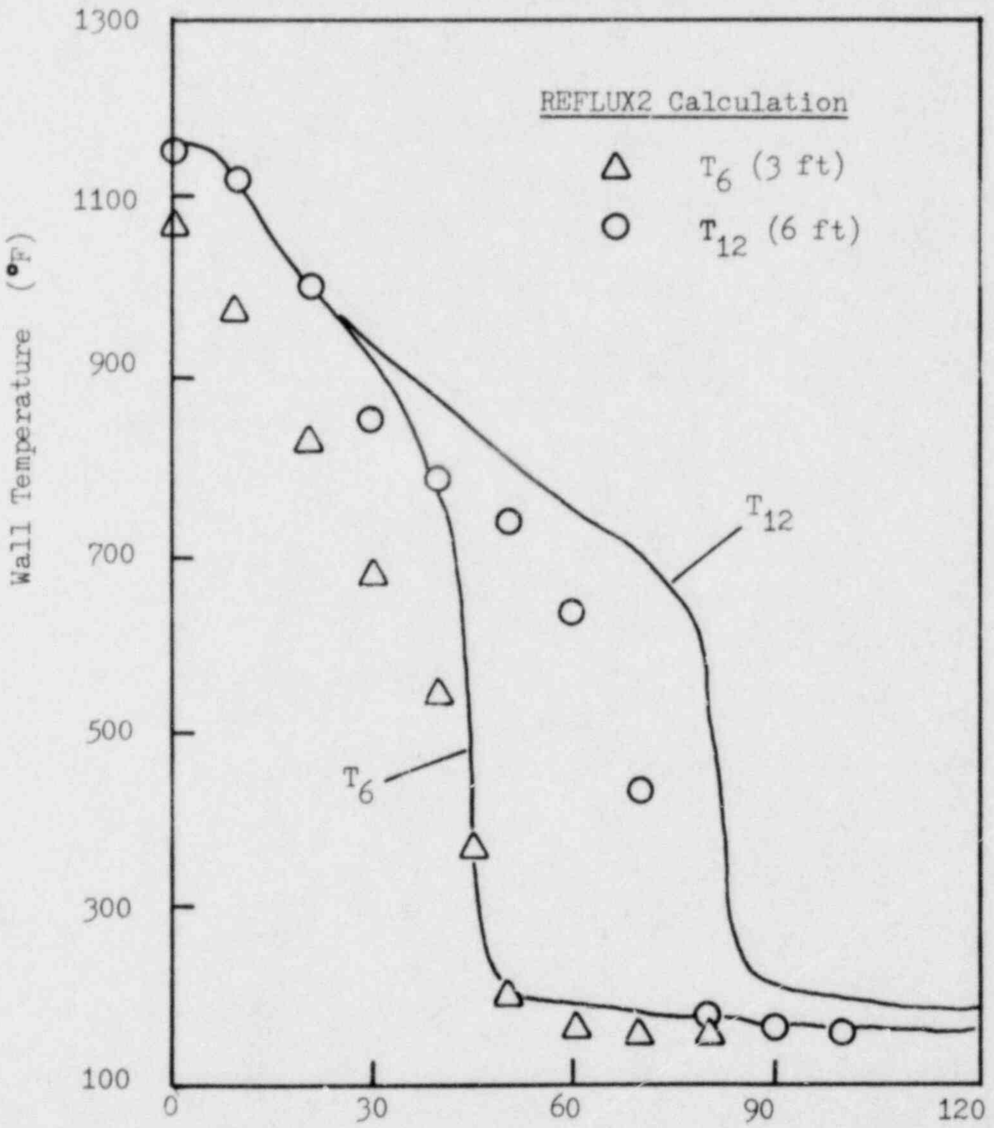

Fig. B.3 Measured and Calculated Wall Temperatures for ANL Run#33

APPENDIX C

LISTING OF COMPUTER PROGRAM

```
      PROGRAM REWET
      REAL KWFT,ME,KC,KF,KOUT
      INTEGER OLEVEL
      DIMENSION QEVAP(1200),Y(7),YNEW(7),FILM(1200)
      COMMON /TEMP/ TEMPW(1200),TEMPC(1200),TEMPF(1200),HTCW(1200)
     1,GROD(1200)
      COMMON/HTC/DTBOIL,DTCHF,DTMIN,HSPL,HFILM,FBA,FBB
      COMMON/ROD/SHBN,SHSS,RHOBN,RHOSS,ACORE,ACLAD,PERG,PERW,HTCG,DT
     1,PF,NSTEP,TF
      COMMON /RK/ YRK(7),FN(7),WINJ,WC,ME,NVAR,WGUP
      COMMON /PRO/ PSYS,TSAT,RHOFS,RHOGS,CPFSAT,CPGSAT,HFG,TSATR,H
      COMMON /GEOM/ AXLD,AXLC,BPL,AD,AC,ABP,AOUT,VOLUP,PER,KC,KF,KOUT
      COMMON /DYNA/ ZD,ZC,WF,PUP,DZEDT,ZE,PE
      COMMON/INJECT/TSHI,FRHI,FRLI,TEMP1,SLOPE1,TIME2,TEMP2,SLOPE2
      COMMON/HOUSE/TEMPH(1200)
      EQUIVALENCE (ZD,Y(1))
      DATA C/4.17E08/,PI/3.1416/
C
C     READ AND WRITE INPUT DATA
C
      READ 2000,NTYPE,NRUN
      IF(NTYPE.EQ.0)PRINT 2001,NRUN
      IF(NTYPE.EQ.1)PRINT 2002,NRUN
      READ 2010,P0,TCOOLI,KWFT,TTSF
      PRINT2010,P0,TCOOLI,KWFT,TTSF
      READ 2020,TSAT,RHOFS,RHOGS,CPFSAT,CPGSAT,HFG
      PRINT2020,TSAT,RHOFS,RHOGS,CPFSAT,CPGSAT,HFG
      READ 2030,DTS,FTIME,NODEC,NODE,INPRNT,NTW1,NTW2,NTW3
      PRINT2030,DTS,FTIME,NODEC,NODE,INPRNT,NTW1,NTW2,NTW3
```

```
      READ 2040,KC,KOUT,AOUT,VFLOOD,FRACT,STEAM
      PRINT2040,KC,KOUT,AOUT,VFLOOD,FRACT,STEAM
      READ 2050,DTBOIL,DTCHF,DTMIN,HSPL,HFILM,FBA,FBB,HVAP
      PRINT2050,DTBOIL,DTCHF,DTMIN,HSPL,HFILM,FBA,FBB,HVAP
      READ 2060,NPIVOT,TCEND,TCP,TWCL
      PRINT2060,NPIVOT,TCEND,TCP,TWCL
      READ 2070,AD,ABP,AC,PER,AXLD,EPL,AXLC,VOLUP
      PRINT2070,AD,ABP,AC,PER,AXLD,EPL,AXLC,VOLUP
      READ 2080,DCLAD,DCORE,SHSS,SHBN,RHOSS,RHOBN,HTCG
      PRINT2080,DCLAD,DCORE,SHSS,SHBN,RHOSS,RHOBN,HTCG
      READ 2090,TSHI,FRHI,FRLI,TEMP1,SLOPE1,TIME2,TEMP2,SLOPE2
      PRINT2090,TSHI,FRHI,FRLI,TEMP1,SLOPE1,TIME2,TEMP2,SLOPE2
      IF(NTYPE.NE.0)GOTO 5
      READ 2100,PERHS,AXHS,RHOHS,CPHS
      PRINT2100,PERHS,AXHS,RHOHS,CPHS
5     CONTINUE
 2000 FORMAT(3I5)
2001  FORMAT(' FLECHT-SET A',I5)
2002  FORMAT(' SEMISCALE MOD3',I5)
 2010 FORMAT(8F10.2)
 2020 FORMAT(8F10.3)
 2030 FORMAT(2F10.3,6I5)
 2040 FORMAT(2F10.2,F10.4,3F10.2)
 2050 FORMAT(6F10.2,E10.3,F10.2)
 2060 FORMAT(I5,3F10.2)
 2070 FORMAT(8F10.4)
 2080 FORMAT(2F10.4,6F10.2)
 2090 FORMAT(8F10.2)
 2100 FORMAT(8F10.4)
C
C     DETERMINE NORMALIZING FACTOR FOR DECAY CURVE & SET AXIAL PROFILE
C
```

```
      DZ=AXLC/FLOAT(NODEC)
      PFSF=PFDK(TTSF)
      QRODI=KWFT*3412./PFSF
      Z=0.0
      DO 10 I=1,NODE
      Z=Z+DZ
   10 QROD(I)=QRODI*PFAX(Z,NTYPE)
C
C     SET INITIAL HOUSING TEMPERATURES
C
      IF(NTYPE.EQ.0)CALL THSI(NODEC)
C
C     SET INITIAL CLAD TEMP AND CORE TEMP WITH TRUNCATED SINE FUNCTION
C
      DELTA=(TCP-TCEND)/FLOAT(NPIVOT)
      TEMPER=TCEND-0.5*DELTA
      DO 20 I=1,NPIVOT
      TEMPER=TEMPER+DELTA
      TEMPW(I)=TEMPER
      TEMPW(NODEC+1-I)=TEMPER
   20 CONTINUE
      NCL=NODEC/2
      BASE=3.1416/FLOAT(NODEC-2*NPIVOT)
      Z=0.5
      J=NPIVOT+1
      DELTA=TWCL-TCP
      DO 30 I=J,NCL
      TEMPER=TCP+DELTA*SIN(Z*BASE)
      TEMPW(I)=TEMPER
```

```
            TEMPW(NODEC+1-I)=TEMPER
      30    Z=Z+1.
            PRINT3000,(TEMPW(I),I=1,NODEC)
    3000    FORMAT(' INITIAL WALL TEMP'//(10F10.1))
            DO 40 I=1,NODE
      40    TEMPC(I)=TEMPW(I)
C
C        INITIALIZE VARIABLES FOR DYNAMIC SOLUTION
            PSYS=P0*144.
            TEMPG=TSAT
            R=85.76
            TSATR=TSAT+460.
            ZC=0.0
            ZD=0.0
            FN(5)=0.0
            WF=0.0
            PUP=PSYS
            DZEDT=0.0
            ZE=0.0
            PE=PSYS
            WG=0.0
            NVAR=4
            LEVEL=0
            TFBP=TCOOLI
            NPRNT=0
            NSTEP=0
            DT=DTS/3600.
            TS=0.0
            TIME=0.0
            VAR1=PER*DZ/(AC*CPFSAT*RHOFS)
            VAR2=PER*DZ/(HFG*RHOGS*AC)
            IF(NTYPE.EQ.0)VAR4=DT*PERHS/(AXHS*RHOHS*CPHS)
```

```
      DHEQ=4.*AC/PER
      NDHEQ=1.+DHEQ/DZ
      QFLOOD=VFLOOD/VAR2*3600.
      VSTR=DZ/DT
      QHS=0.0
      PERW=PI*DCLAD/12.
      PERG=PI*DCORE/12.
      ACORE=PI*DCORE*DCORE/(4.*144.)
      ACLAD=PI*DCLAD*DCLAD/(4.*144.)-ACORE
      COF=0.0
      COG=0.0
      DO 50 I=1,NODE
   50 TEMPF(I)=TEMPG
C
C     START TIME LOOP
C
  100 CONTINUE
      NSTEP=NSTEP+1
      NPRNT=NPRNT+1
      TS=TS+DTS
      TIME=TS/3600.
      WINJ=FLOWIN(TS)
      PF=PFDK(TS+TTSF)
      ZEOLD=ZE
      DZEOLD=DZEDT
      WFOLD=WF
      WGUP=STEAM
      HVAPOR=HVAP
      IF(TS.GT.10.)GOTO 105
```

```
      WGUP=STEAM*TS/10.
      HVAPOR=HVAP*TS/10.
105   CONTINUE
C
C     RENEW STATE VARIABLES BY RUNGE KUTTA METHOD
C     TIME STEP IS REDUCED IN CASE OF ENTRAINMENT
C
      ITR=10
      IF(NVAR.EQ.7)ITR=100
      XITR=ITR
      DT=DTS/(3600.*XITR)
      DO 160 J=1,ITR
      DO 110 I=1,NVAR
  110 YRK(I)=Y(I)
      CALL RUNGE
      DO 120 I=1,NVAR
      FDT=FN(I)*DT
      YRK(I)=Y(I)+0.5*FDT
  120 YNEW(I)=Y(I)+FDT/6.
      CALL RUNGE
      DO 130 I=1,NVAR
      FDT=FN(I)*DT
      YRK(I)=Y(I)+0.5*FDT
  130 YNEW(I)=YNEW(I)+FDT/3.
      CALL RUNGE
      DO 140 I=1,NVAR
      FDT=FN(I)*DT
      YRK(I)=Y(I)+FDT
  140 YNEW(I)=YNEW(I)+FDT/3.
      CALL RUNGE
      DO 150 I=1,NVAR
      YNEWI=YNEW(I)+FN(I)*DT/6.
```

```
      FN(I)=(YNEWI-Y(I))/DT
150     Y(I)=YNEWI
160     CONTINUE
      DT=DTS/3600.
C
C     END RUNGE-KUTTA METHOD,START THERMAL CALCULATIONS
C
      IF(ZD.GT.AXLD)ZD=AXLD
      OLEVEL=LEVEL
      LEVEL=IFIX(ZC/DZ)
      IF(LEVEL.LT.0)LEVEL=0
      VF=WF/(AC*RHOFS)
      IF(LEVEL.GE.NODE)LEVEL=NODE-1
C
C COMPUTE ACCELERATION PRESSURE DROP AND DIFFERENTIAL PRESSURES
C ACROSS DOWNCOMER AND CORE
C
      ACCEL=(WF-WFOLD)/(DT*G*RHOFS*AC)
      FRICT=0.5*KC*VF*ABS(VF)/(G*(ZD+ZC))
      DPD=ZD*(1.-ACCEL*AC/AD-FRICT)
      DPC=ZC*(1.+ACCEL+FRICT)+(PE-PUP)/RHOFS
      DPLOOP=(PUP-PSYS)/RHOFS
C
C    CHECK IF ENTRAINED LIQUID HAS REACHED MAXIMUM VELOCITY
C
      IF(ZE.EQ.0.0.OR.(DZEDT-DZEOLD).GT.0.0)GOTO 180
      IF(DZEDT.GT.0.0)GOTO 165
      ZE=0.0
      DZEDT=0.0
```

```
            ZC=ZC+EXPEL
            COF=COF-ME
            GOTO 170
 165        CONTINUE
            DZEDT=DZEOLD
            ZE=ZEOLD+DZEDT*DT
   170      NVAR=4
            PE=PUP
   180      CONTINUE
C
C       CALCULATE HEAT TRANSFER IN VAPOR FLOW REGION AND UPDATE
C       ROD TEMPERATURES
C
            QVAPOR=0.0
            J=LEVEL+1
            DO 270 I=J,NODE
            HTCW(I)=HVAPOR
            TF=TSAT
            QVAPOR=QVAPOR+HVAPOR*(TEMPW(I)-TSAT)
            CALL TROD(I)
 270        CONTINUE
C
C       CALCULATE FLUID TEMP WITH AN IMPLICIT BACKWARD DIFF METHOD
C
            IF(LEVEL.LT.1)GOTO 360
            IF(VF.LT.0.0)GOTO 310
            LV=0
            LS=1
            VFABS=VF
            TFBP=TCOOL(TS)
            TFNEW=TFBP
            GOTO 320
```

```
      310   LV=LEVEL+1
            LS=-1
            VFABS=-VF
            TFNEW=TEMPF(OLEVEL)
      320   CONTINUE
            DO 350 J=1,LEVEL
            I=(J-LV)*LS
            TFOLD=TEMPF(I)
            IF(TFOLD.GT.TSAT)TFOLD=TFNEW
C
C     DETERMINE HOUSING HTC'S & UPDATE HOUSING TEMP'S
C
            IF(NTYPE.NE.0)GOTO 322
            DTSATH=TEMPH(I)-TSAT
            HTCH=BOIL(DTSATH)
            TF=TSAT
            IF(DTSATH.LT.DTBOIL)TF=TFOLD
            THS=(TEMPH(I)+VAR4*HTCH*TF)/(1.+VAR4*HTCH)
            TEMPH(I)=THS
            QHS=HTCH*(THS-TF)*PERHS/PER
 322          CONTINUE
C
C     DETERMINE HTC'S IN LIQUID REGION AND UPDATE ROD TEMP
C
            DTSAT=TEMPW(I)-TSAT
            HTCW(I)=BOIL(DTSAT)
            TF=TSAT
            IF(DTSAT.LT.DTBOIL)TF=TFOLD
            CALL TROD(I)
```

```
      IF(DTSAT.GT.DTBOIL)GOTO 325
      QW=HTCW(I)*(TEMPW(I)-TFOLD)+QHS
      QEVAP(I)=0.0
      GOTO 326
  325 QW=HTCW(I)*(TEMPW(I)-TSAT)+QHS
      IF(TFOLD.EQ.TSAT.AND.TFNEW.EQ.TSAT)GOTO 340
C
C     ASSUME 10% OF QW GENERATES VAPOR IN SUBCOOLED BOILING
C
      QEVAP(I)=0.1*QW/(1.+CPFSAT*(TSAT-TFOLD)/HFG)
      QW=0.9*QW
  326 CONTINUE
      TFNEW=(QW*VAR1+TFOLD*VSTR+TFNEW*VFABS)/(VFABS+VSTR)
      IF(TFNEW.LE.TSAT)GOTO 350
      QW=(TFNEW-TSAT)*(VFABS+VSTR)/VAR1+QEVAP(I)
      TFNEW=TSAT
  340 QEVAP(I)=QW
  350 TEMPF(I)=TFNEW
      IF(VF.GE.0.0)GOTO 360
      TFBP=TFBP-WF*VAR3*(TFNEW-TCOOLI)
      IF(TFBP.GT.TSAT)TFBP=TSAT
  360 CONTINUE
      J=LEVEL+1
      DO 370 I=J,NODE
  370 TEMPF(I)=TEMPG
C
C     TEST FOR LIQUID ENTRAINMENT AND EXPULSION
C
      QSUM=0.0
      NCHECK=1
      IF(LEVEL.GT.0)GOTO 405
      PE=PUP
```

```
      IF(ZE.LT.AXLC)GOTO 450
      ZE=0.0
      DZEDT=0.0
      NVAR=4
      GOTO 450
  405 CONTINUE
      IF(ZE.EQ.0.0.OR.ZE.GT.AXLC)GOTO 420
      DO 410 I=1,LEVEL
  410 QSUM=QSUM+QEVAP(I)
      GOTO 450
  420 DO 430 I=1,LEVEL
      QSUM=QSUM+QEVAP(I)
      IF(QSUM.LT.QFLOOD.OR.NCHECK.EQ.0)GOTO 430
      DTSAT=TEMPW(I)-TSAT
      IF(DTSAT.LT.DTMIN.AND.(LEVEL-I).GE.NDHEQ)GOTO 440
      NCHECK=0
  430 CONTINUE
      ZE=0.0
      DZEDT=0.0
      PE=PUP
      NVAR=4
      GOTO 450
  440 EXPEL=FRACT*(ZC-FLOAT(I)*DZ)
      ZC=ZC-EXPEL
      ME=EXPEL*AC*RHOFS
      LEVEL=I
      ZE=ZC+DHEQ
      DZEDT=FN(2)
      PE=PUP+ME/AC
```

```
          NVAR=7
          COF=COF+ME
    450   WG=(QSUM+QVAPOR)*PER*DZ/HFG
          WVAPOR=QVAPOR*PER*DZ/HFG
          COG=COG+WG*DT
C
C       OUTPUT
C
          IF(NPRNT.LT.INPRNT)GOTO 1500
          NPRNT=0
          J=LEVEL
          IF(LEVEL.EQ.0)J=1
          PUPSI=PUP/144.
          PESI=PE/144.
          VFPS=WF/(RHOFS*AC*3600.)
          VGPS=WG/(RHOGS*AC*3600.)
          DZEDTS=DZEDT/3600.
          WRITE(9,3020)TS,DPD,DPC,ZD,ZC,DPLOOP,VGPS,TEMPW(NTW1)
          1,TEMPW(NTW2),TEMPW(NTW3)
  3020      FORMAT(1X,7F7.2,3F7.1)
          PRINT3010,TS,ZD,ZC,VFPS,VGPS,ZE,DZEDTS,PUPSI,PESI,TEMPC(J)
          1 ,TEMPW(J),TEMPF(J),TEMPH(J),HTCW(J),COF,COG,LEVEL
   3010   FORMAT(1X,6F7.2,8F7.1,2F7.2,I5)
   1500   IF(TS.LT.FTIME)GOTO 100
          STOP
          END
```

```
      SUBROUTINE RUNGE
C
C     SOLVES DYNAMIC EQUATIONS WITH RUNGE-KUTTA METHOD
C
      REAL ME,KC,KF,KOUT
      COMMON /RK/ ZD,ZC,WF,PUP,DZEDT,ZE,PE,FN(7),WINJ,WG,ME,NVAR,WGUP
      COMMON /GEOM/ AXLD,AXLC,BPL,AD,AC,ABP,AOUT,VOLUP,PER,KC,KF,KOUT
      COMMON /PRO/ PSYS,TSAT,RHOFS,RHOGS,CPFSAT,CPGSAT,HFG,TSATR,R
      DATA G/4.17E08/
      DP=PUP-PSYS
      RHOG=RHOGS
      IF(DP)10,20,30
   10 WOUT=-AOUT*(-2.*RHOG*G*DP/KOUT)**0.5
      GOTO 40
   20 WOUT=0.0
      GOTO 40
   30 WOUT=AOUT*(2.*RHOG*G*DP/KOUT)**0.5
   40 CONTINUE
      FN(1)=(WINJ-WF)/(RHOFS*AD)
      FN(2)=(WF-WG)/(RHOFS*AC)
      IF(NVAR.EQ.7)GOTO 50
      P=PUP
      WV=WG+WGUP
      DZDT=FN(2)
      GOTO 60
   50 CONTINUE
      FN(5)=(PE-PUP)*G*AC/ME-G
      FN(6)=DZEDT
      FN(7)=(WG*R*TSATR-PE*AC*(DZEDT-FN(2)))/(AC*(ZE-ZC))
      P=PE
      WV=WGUP
      DZDT=DZEDT
   60 CONTINUE
      FN(3)=((PSYS-P+RHOFS*(ZD-ZC))*G-0.5*KC*WF*ABS(WF)/(RHOFS*AC*AC))
     1 /(ZD/AD+BPL/ABP+ZC/AC)
      FN(4)=((WV-WOUT)*R*TSATR+PUP*AC*DZDT)/VOLUP
      RETURN
      END
```

```
      SUBROUTINE TROD(I)
C
C     UPDATES ROD TEMPS WITH A 2-NODE, RADIAL-CONDUCTION-ONLY MODEL
C
      COMMON /TEMP/ TEMPW(1200),TEMPC(1200),TEMPF(1200),HTCW(1200)
     1,QROD(1200)
      COMMON/ROD/SHBN,SHSS,RHOBN,RHOSS,ACORE,ACLAD,PERG,PERW,HTCG,DT
     1 ,PF,NSTEP,TF
      IF(NSTEP.GT.1)GOTO 10
      CC=SHBN*RHOBN*ACORE
      CW=SHSS*RHOSS*ACLAD
      CCDT=CC/DT
      CWDT=CW/DT
      B=-HTCG*PERG
      A=CCDT-B
      D=B
      BD=B*D
   10 CONTINUE
      HWPW=HTCW(I)*PERW
      C=QROD(I)*PF+CCDT*TEMPC(I)
      E=CWDT-B+HWPW
      F=HWPW*TF+CWDT*TEMPW(I)
      DET=A*E-BD
      TEMPC(I)=(C*E-B*F)/DET
      TEMPW(I)=(A*F-C*D)/DET
      RETURN
      END
```

```
      FUNCTION PFDK(TTS)
C
C    THIS SUBROUTINE CALCULATE THE DECAY HEAT POWER FACTOR ACCORDING
C    ANS STANDARD + 20%
C    ADAPTED FROM THE REFLUX CODE
C
      IF(TTS.GT.10.0)GOTO 010
      A=0.0603
      B=0.0639
      GOTO 099
  010 IF(TTS.GT.150.0)GOTO 020
      A=0.0766
      B=0.181
      GOTO 099
  020 A=0.130
      B=0.283
  099 PU=0.001632*EXP(-0.000491*TTS)
      PNP=0.001596*(0.006994*(EXP(-3.41E-06*TTS)-EXP(-0.000491*TTS))
     1 +EXP(-3.41E-06*TTS))
      PFDK=1.2*A*TTS**(-B)+1.1*(PU+PNP)
      RETURN
      END

      FUNCTION BOIL(DTSAT)
C
C     DETERMINES HEAT TRANSFER COEFFICIENTS FROM BOILING CURVE
C
      COMMON/HTC/DTBOIL,DTCHF,DTMIN,HSPL,HFILM,FBA,FBB
      IF(DTSAT.GT.DTBOIL)GOTO 10
      BOIL=HSPL
      GOTO 100
   10 IF(DTSAT.GT.DTCHF)GOTO 20
      BOIL=0.07*DTSAT**2.86
      GOTO 100
   20 BOIL=FBA*EXP(FBB*DTSAT)+HFILM/DTSAT**0.25
  100 RETURN
      END
```

```
      FUNCTION PFAX(AX,NTYPE)
C
C     THIS SUBROUTINE SPECIFIES THE AXIAL POWER PROFILE
C     FOR THE SEMISCALE MOD-3 AND FLECHT-SET TESTS
C
      Z=AX
      IF(Z.GT.6.)Z=12.-Z
      IF(NTYPE.EQ.0)GOTO 100
C
C     SEMISCALE MOD-3
C
      IF(Z.GT.1.)GOTO 10
      PFAX=0.31/1.55
      GOTO 60
10      IF(Z.GT.2.)GOTO 20
      PFAX=0.59/1.55
      GOTO 60
20      IF(Z.GT.3.)GOTO 30
      PFAX=0.89/1.55
      GOTO 60
30      IF(Z.GT.4.)GOTO 40

      PFAX=1.22/1.55
      GOTO 60
40      IF(Z.GT.5.)GOTO 50
      PFAX=1.44/1.55
      GOTO 60
50      PFAX=1.55/1.55
60      RETURN
```

```
C
C        FLECHT-SET
C
  100    CONTINUE
         IF(Z.GT.1.8)GOTO 110
         PFAX=0.26681
         GOTO 200
  110    IF(Z.GT.2.4)GOTO 120
         PFAX=0.42193
         GOTO 200
  120    IF(Z.GT.3.0)GOTO 130
         PFAX=0.54602
         GOTO 200
  130    IF(Z.GT.3.6)GOTO 140
         PFAX=0.67937
         GOTO 200
  140    IF(Z.GT.4.2)GOTO 150
         PFAX=0.79566
         GOTO 200
  150    IF(Z.GT.4.8)GOTO 160
         PFAX=0.91195
         GOTO 200
  160    IF(Z.GT.5.4)GOTO 170
         PFAX=0.94169
         GOTO 200
  170    PFAX=0.977
  200    RETURN
         END
```

```
      FUNCTION FLOWIN(TS)
C
C    RETURNS INJECTION FLOW RATE IN LB/HR
C
      COMMON/INJECT/TSHI,FRHI,FRLI,TEMP1,SLOPE1,TIME2,TEMP2,SLOPE2
      IF(TS.GT.TSHI)GOTO 10
      FLOWIN=FRHI*3600.
      RETURN
   10 FLOWIN=FRLI*3600.
      RETURN
      END
      FUNCTION TCOOL(TS)
C
C     RETURNS INLET COOLANT TEMPERATURE
C
      COMMON/INJECT/TSHI,FRHI,FRLI,TEMP1,SLOPE1,TIME2,TEMP2,SLOPE2
      IF(TS.GT.TIME2)GOTO 10
      TCOOL=TEMP1+SLOPE1*TS
      RETURN
 10   TCOOL=TEMP2+SLOPE2*(TS-TIME2)
      RETURN
      END
```

```
      SUBROUTINE THSI(NODEC)
C
C     INITIALIZES HOUSING TEMPS; USED IN FLECHT-SET RUNS ONLY
C
      COMMON/HOUSE/TEMPH(1200)
      INT=NODEC/6
      XINT=INT
      READ 1000,THBP,TEMPH(INT),TEMPH(2*INT),TEMPH(3*INT),TEMPH(4*INT)
     1,TEMPH(5*INT),TEMPH(6*INT)
 1000 FORMAT(8F10.2)
      TH2=THBP
      N=0
      DO 50 I=1,6
      TH1=TH2
      TH2=TEMPH(N+INT)
      DTH=(TH2-TH1)/XINT
      DO 50 J=1,INT
      N=N+1
      TH1=TH1+DTH
   50 TEMPH(N)=TH1
      RETURN
      END
```

NRC FORM 335 (7-77) U.S. NUCLEAR REGULATORY COMMISSION

BIBLIOGRAPHIC DATA SHEET

1. REPORT NUMBER (Assigned by DDC): NUREG/CR-1314

4. TITLE AND SUBTITLE (Add Volume No., if appropriate)

Gravity Reflood Oscillations in a Pressurized Water Reactor

2. (Leave blank)

3. RECIPIENT'S ACCESSION NO.

7. AUTHOR(S)

Y. L. Cheung and P. Griffith

5. DATE REPORT COMPLETED

MONTH	YEAR
December	1979

DATE REPORT ISSUED

MONTH	YEAR
February	1980

9. PERFORMING ORGANIZATION NAME AND MAILING ADDRESS (Include Zip Code)

Department of Mechanical Engineering
Massachusetts Institute of Technology
Boston, Massachusetts

6. (Leave blank)

8. (Leave blank)

12. SPONSORING ORGANIZATION NAME AND MAILING ADDRESS (Include Zip Code)

U.S. Nuclear Regulatory Commission
Division of Reactor Safety Research
Washington, D. C. 20555

10. PROJECT/TASK/WORK UNIT NO.

11. CONTRACT NO.

FIN A4060

13. TYPE OF REPORT

Technical Report

PERIOD COVERED (Inclusive dates)

15. SUPPLEMENTARY NOTES

14. (Leave blank)

16. ABSTRACT (200 words or less)

The thermal hydraulics of reflood oscillations in a pressurized water reactor is studied. Violent steam generation beneath the core water level and subsequent expulsion of the coolant are proposed as the physical mechanisms responsible for driving the oscillations. A computer model of the gravity reflood process is formulated based on a simplified boiling curve and one dimensional fluid mechanics. In general, model calculations compare favorably with experiments. The core coolant level, however, cannot be calculated with certainty because the model does not account, in sufficient details, for interactions beyond the reactor core. Calculated vapor velocities at the core exit indicate that draining of carryover coolant from the upper plenum is possible.

17. KEY WORDS AND DOCUMENT ANALYSIS

17a. DESCRIPTORS

17b. IDENTIFIERS/OPEN-ENDED TERMS

18. AVAILABILITY STATEMENT

Unlimited

19. SECURITY CLASS (This report): Unclassified

20. SECURITY CLASS (This page)

21. NO. OF PAGES

22. PRICE
$

UNITED STATES
NUCLEAR REGULATORY COMMISSION
WASHINGTON, D. C. 20555

OFFICIAL BUSINESS
PENALTY FOR PRIVATE USE, $300

POSTAGE AND FEES PAID
U.S. NUCLEAR REGULATORY
COMMISSION

U.S. MAIL

120555031837 2 ANR2 P-016
US NRC
SECY PUBLIC DOCUMENT ROOM
BRANCH CHIEF
HST LOBBY
WASHINGTON DC 20555

POOR ORIGINAL